explored. Embryonic stem cells (ESCs) or iPSCs have the capacity for self-renewal while maintaining pluripotency (Takahashi et al., 2007) and could potentially form the basis for the unlimited induction of antigen-specific juvenile T cells. However, there are challenges to this approach as well, given that methods for the differentiation and immunological education of ESCs and iPSCs, or indeed that of intermediate hematopoietic stem and/or progenitor cells, into fully matured functional human T cells are not well established (Timmermans et al., 2009). Reprogramming the nuclei of lymphocytes was historically performed for studying whether terminally differentiated or fully matured somatic cells could revert to a pluripotent state. The first demonstration of lymphocyte reprogramming employed somatic cell nuclear transfer in murine B and T cells, proving that terminally differentiated somatic cells were reprogrammable (Hochedlinger and Jaenisch, 2002). Reprogramming murine B cells into pluripotent stem cells by iPSC technology also provided definite proof for fate reversibility in fully matured somatic cells (Hanna et al., 2008). From another point of view, nuclear reprogramming of lymphocytes is seen as having applications for regenerative medicine different than those for scientific research. The irreversible rearrangement of genes encoding immunoglobulins and TCRs was recognized solely as a genetic marker in somatic cell nuclear transfer and iPSC research. However, the preserved rearrangements in genomic DNA can also provide a blueprint of "educated" weapons for attacking cancers and pathogens in adoptive immunotherapy. Although several groups have reported the generation of T cell-derived iPSCs (T-iPSCs), their clinical applications have yet to be thoroughly explored (Brown et al., 2010; Loh et al., 2010; Seki et al., 2010; Staerk et al., 2010).

In the present study, we chose a T cell clone specific to an HIV type 1 (HIV-1) epitope of known structure to act as a generic representation of iPSC-mediated T cell regeneration. We successfully induced iPSCs from antigen-specific T cells and redifferentiated them into functional T cells. This may act as proof of concept for the application of "rejuvenated" T cells in treating various diseases. Crucial to this concept was that T-iPSCs retained the assembled "endogenous" TCR genes even after being subjected to nuclear reprogramming. Furthermore, redifferentiated T cells showed the same pattern of TCR gene arrangement as that in the original T cells. These features may therefore serve as the foundation for the reproduction of unlimited numbers of T cells that express desired TCRs conferring to antigen specificity.

RESULTS

Reprogramming an Antigen-Specific Cytotoxic T Cell Clone into Pluripotency

To establish T cell-derived iPSCs, we magnetically separated the $CD3^+$ T cell population from peripheral blood mononuclear cells (PBMCs) of healthy volunteers. The isolated $CD3^+$ T cells were stimulated with human CD3 and CD28 antibody-coated microbeads (α-CD3/28 beads) in the presence of interleukin-2 (IL-2). We then transduced the activated $CD3^+$ T cells with separate retroviral vectors that individually code for *OCT3/4*, *SOX2*, *KLF4*, and c-*MYC*. Human ESC-like colonies were obtained within 25 days of culture (Figure S1A available online).

We also isolated PBMCs from an HLA-A24-positive patient with a chronic HIV-1 infection. $CD8^+$ CTL clones specific for an antigenic peptide (amino acids [aa] 138–145) from the HIV-1 Nef protein (Nef-138-8(WT); RYPLTFGW) (Altfeld et al., 2006) were established. One of the clones, H25-#4, was stimulated using α-CD3/28 beads in the presence of IL-2 and then transduced simultaneously with six retroviral vectors encoding *OCT3/4*, *SOX2*, *KLF4*, c-*MYC*, *NANOG*, and *LIN28A*. However, we could not reprogram H25-#4 into pluripotency, possibly due to the cells being in a low infectious and exhausted state, or due to insufficient expression of the reprogramming factors. In response, we attempted to increase transduction efficiency and transgene expression by using two Sendai virus (SeV) vectors. One of them encodes tetracistronic factors (*OCT3/4*, *SOX2*, *KLF4*, and c-*MYC*) (Nishimura et al., 2011) with the miR-302 target sequence (SeVp[KOSM302L]; K.N., M.O., and M.N., data not shown), and another encodes SV40 large T antigen (SeV18[T]) (Fusaki et al., 2009). After transduction of phytohemagglutinin (PHA)-activated H25-#4 cells with the SeV vectors in the presence of IL-7 and IL-15, sufficient numbers of human ESC-like colonies appeared within 40 days of culture (Figure 1A). Use of this SeV system and optimization of transduction conditions greatly improved the reprogramming efficiency. It enabled us to reprogram several $CD8^+$ or $CD4^+$ T cell clones specific to pp65 antigen in cytomegalovirus (CMV), glutamic acid decarboxylase (GAD) antigen in type 1 diabetes, and α-GalCer (Table 1).

The resultant $CD3^+$ T cell- and H25-#4-derived ESC-like colonies (TkT3V1-7 and H254SeVT-3, respectively) exhibited alkaline phosphatase (AP) activity and expressed the pluripotent cell markers SSEA-4, Tra-1-60, and Tra-1-81 (Figures S1B–S1E and 1B–1E). H254SeVT-3 expressed HLA-A24 (Figure 1F). Both TkT3V1-7 and H254SeVT-3 also expressed human ESC-related genes (Figures S1F and 1G). The expression of exogenous reprogramming factors from the integrated provirus (TkT3V1-7) was halted (Figure S1F), and nonintegrated SeV genomic RNA was successfully removed from the cytosol by RNAi or by self-degradation caused by temperature-sensitive mutations (H254SeVT-3) (Figure 1H). Comparison of gene-expression profiles revealed that the gene-expression patterns in the ESC-like cells were similar to those in human ESCs, but differed significantly from those in peripheral blood (PB) T cells (Figure S1G). Scant methylation of the *OCT3/4* and *NANOG* promoter regions was confirmed using bisulfite PCR, thus indicating successful reprogramming (Freberg et al., 2007) (Figures S1H and 1I). In addition, when injected into nonobese diabetic severe combined immunodeficient (NOD-Scid) mice, those cells formed teratomas containing characteristic tissues derived from all three germ layers, which is indicative of pluripotency (Brivanlou et al., 2003) (Figures S3 and 2A). Therefore, those colonies were confirmed as typical human iPSCs.

T-iPSCs Carry Preassembled TCR Genes from the Original T Cell

Almost all TCRs are composed of heterodimerically associated α and β chains. *TCRA* or *TCRB* gene (encoding α chain or β chain, respectively) rearrangements are involved in normal αβ T cell development in the thymus. These rearrangements enabled us to determine retrospectively whether the iPSCs were derived from an αβ T cell. The BIOMED-2 consortium designed multiplex-PCR primers for analyzing *TCRB* gene assemblies (van Dongen et al., 2003), and we designed the primers for detecting *TCRA*

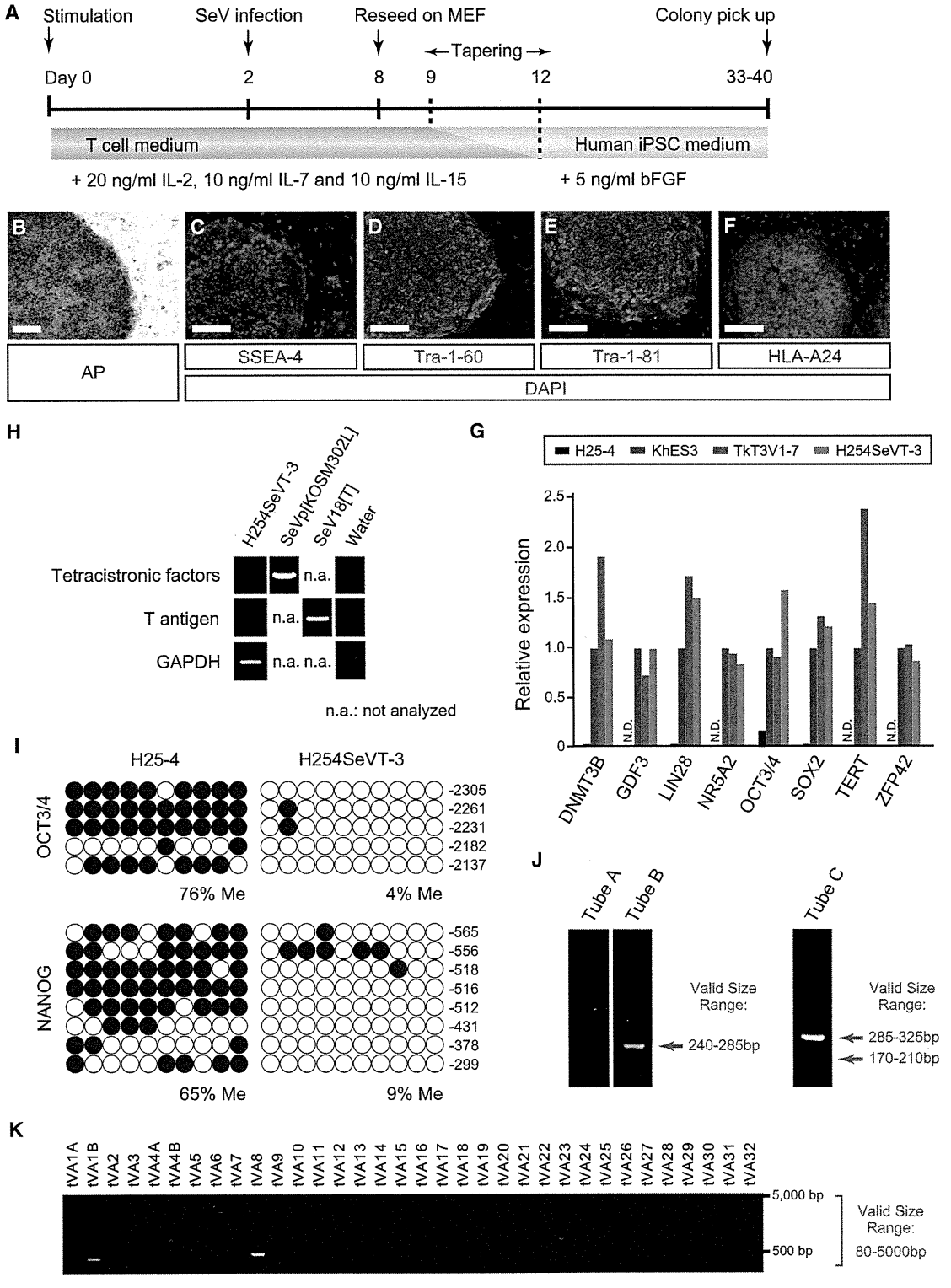

Figure 1. Generation of Human iPSCs from a CTL Clone

(A) Schematic illustration showing the generation of T-iPSCs from H25-#4 T cells using SeV vectors encoding polycistronic *OCT3/4*, *SOX2*, *KLF4*, and c-*MYC*, or SV40 large T antigen. The "tapering" indicates the gradual replacement of culture medium with human iPSC medium.

(B–F) AP activity (B) and expression of pluripotency markers (SSEA-4, C; Tra-1-60, D; and Tra-1-81, E) and HLA-A24 (F) in H254SeVT-3 cells. Nuclei were counterstained with DAPI. The scale bar represents 200 μm.

(G) Quantitative PCR for pluripotency genes in H25-#4, KhES3, TkT3V1-7, and H254SeVT-3 cells. Individual PCR reactions were normalized against 18S ribosomal RNA (rRNA).

(legend continued on next page)

Table 1. Generation of Human T-iPSCs from Various Patient-Derived T Cell Specimens

Antigen	T Cell Source	Initial Cell Number	No. of ESC-like Colonies	No. of Colonies Picked up for Establishing T-iPSC Clones	Date (MM/YYYY)
HIV-1 Nef	monoclonal T cell clone	4×10^5	7	7	05/2011
CMV pp65	polyclonal tetramer-sorted cells	~5,000	15	15	07/2011
GAD	monoclonal T cell clone	1×10^6	>100	not picked up	08/2012
		5×10^5	>100	19	08/2012
α-GalCer	FACS-sorted Vα24$^+$ cells	1×10^6	>100	not picked up	08/2012
		5×10^5	>100	7	08/2012

Sample cells were transduced with *OCT3/4*, *SOX2*, *KLF4*, *c-MYC*, and SV40 large T-antigen by using two Sendai virus (SeV) vectors (SeVp [KOSM302L] and SeV18[T]). After around 40 days, the number of embryonic stem cell (ESC)-like colonies were counted on the basis of morphology and alkaline phosphatase (AP) activity. All established T cell-derived induced pluripotent stem cell (T-iPSC) lines were free from residual SeV vectors (one example in the case of the HIV-1 Nef-specific T-iPSC clone is shown in Figure 1H). CMV, cytomegalovirus; GAD, glutamic acid decarboxylase; FACS, fluorescence-activated cell sorting.

gene assemblies (Figure S2). *TCRB* and *TCRA* gene assemblies were identified as single bands representing each allele in TkT3V1-7 and H254SeVT-3 (Figures S1H, S1I, 1J, and 1K).

We next confirmed the presence of an antigen-recognition site on the TCR that consisted of three complementarity-determining regions (CDR1, CDR2, and CDR3). CDR3 is the most diversifiable among the three because it spans the V(D)J-junction region, where several random nucleotides (N or P nucleotides) are inserted (Alt and Baltimore, 1982; Lafaille et al., 1989). We determined the CDR3 sequences of the assembled *TCRA* and *TCRB* genes in TkT3V1-7 and H254SeVT-3 and identified a set of productive *TCRA* and *TCRB* gene rearrangements (i.e., in-frame junction with no stop codon) (Table S1 and Table 2). Furthermore, the sequences of CDR3 from H254SeVT-3 and H25-#4 were completely identical at both *TCRA* and *TCRB* gene loci. These results indicated that the iPSCs established were derived from a single T cell and that the antigen specificity encoded in the genomic DNA of the T cell was conserved during reprogramming.

Redifferentiation of T-iPSCs into CD8 Single-Positive T Cells Expressing the Desired TCR

Following the application of specific in vitro differentiation protocols, iPSCs can give rise to mesoderm-derived cell types, especially hematopoietic stem and/or progenitor cells (Takayama et al., 2008; Vodyanik et al., 2005) (Figure 2B). This was applied to assess the capacity of T-iPSCs for hematopoietic differentiation by coculturing on C3H10T1/2 feeder cells in the presence of VEGF, SCF, and FLT-3L for the generation of CD34$^+$ hematopoietic stem and/or progenitor cells. On day 14 of culture, the cells were transferred onto Delta-like 1-expressing OP9 (OP9-DL1) feeder cells (Timmermans et al., 2009) and were cocultured in the presence of FLT-3L and IL-7 (Ikawa et al., 2010) (Figure 2B). After 21–28 days of culture, the hematopoietic cells differentiated into CD45$^+$, CD38$^+$, CD7$^+$, CD45RA$^+$, CD3$^+$, and TCRαβ$^+$ T lineage cells (Figure S4). As was the case with TCRαβ transgenic mice (Borgulya et al., 1992) and chimeric mice derived from ESCs produced through nuclear transplantation of T cells (Serwold et al., 2007), aberrant expression of TCRαβ was observed at the CD4/CD8 double-negative (DN) stage. Although some of these T lineage cells differentiated into the CD4/CD8 double-positive (DP) stage and the more mature CD4 or CD8 single-positive (SP) stages (Figure 2C), we could not characterize the small number of SP cells in more detail.

During thymocyte development, the CD4/CD8 DN and DP stages correspond respectively to the *TCRB*-encoded β chain and *TCRA*-encoded α chain assembly stages (von Boehmer, 2004). In the *TCRB* locus, the negative-feedback regulation of gene assembly and the capacity to deter further rearrangement are very strict (Khor and Sleckman, 2002). In the *TCRA* locus, by contrast, negative-feedback regulation is relatively loose, and further gene assembly of the preassembled gene, a phenomenon known as "receptor revision," tends to occur (Huang and Kanagawa, 2001; Krangel, 2009). In experiments using TCRα transgenic mice, the reactivation of *Rag1* and *Rag2*, genes related to recombination machinery, occurred in CD4/CD8 DP-stage thymocytes, and gene assembly of endogenous *Tcra* was observed (Padovan et al., 1993; Petrie et al., 1993). Such further gene assembly would be exceedingly undesirable for our purposes, because it would probably convert the tropism of the TCR and render the redifferentiated T cells incapable of attacking the previously targeted antigen. To determine whether such receptor revision could occur in redifferentiating T lineage cells, we collected CD1a$^-$ DN- and CD1a$^+$ DP-stage cells from among the CD45$^+$, CD3$^+$, TCRαβ$^+$, and CD5$^+$ T lineage cells and then analyzed the gene rearrangement of TCR messenger RNAs (mRNAs) (Figures S5A–S5C). Nucleotide sequences of *TCRB* mRNAs in the T lineage cells were identical to those in

(H) Detection of the remnants of SeV genomic RNAs by RT-PCR. Each column represents the template cDNA synthesized from H254SeVT-3 cells, SeVp [KOSM302L] virus solution, and SeV18[T] virus solution. cDNAs from virus solution were the positive controls.
(I) Bisulfite sequencing analyses of the *OCT3/4* and *NANOG* promoter regions in H25-#4 and H254SeVT-3 cells. White and black circles represent unmethylated and methylated (Me) CpG dinucleotides, respectively.
(J) Multiplex PCR analysis to detect *TCRB* gene rearrangements in the H254SeVT-3 genome. Tubes A and B contain Vβ-(D)Jβ assemblies; Tube C contains D-Jβ assemblies.
(K) Multiplex PCR analysis for detection of *TCRA* gene rearrangements (V-Jα assemblies).
See Figures S1, S2, and S3 for additional data.

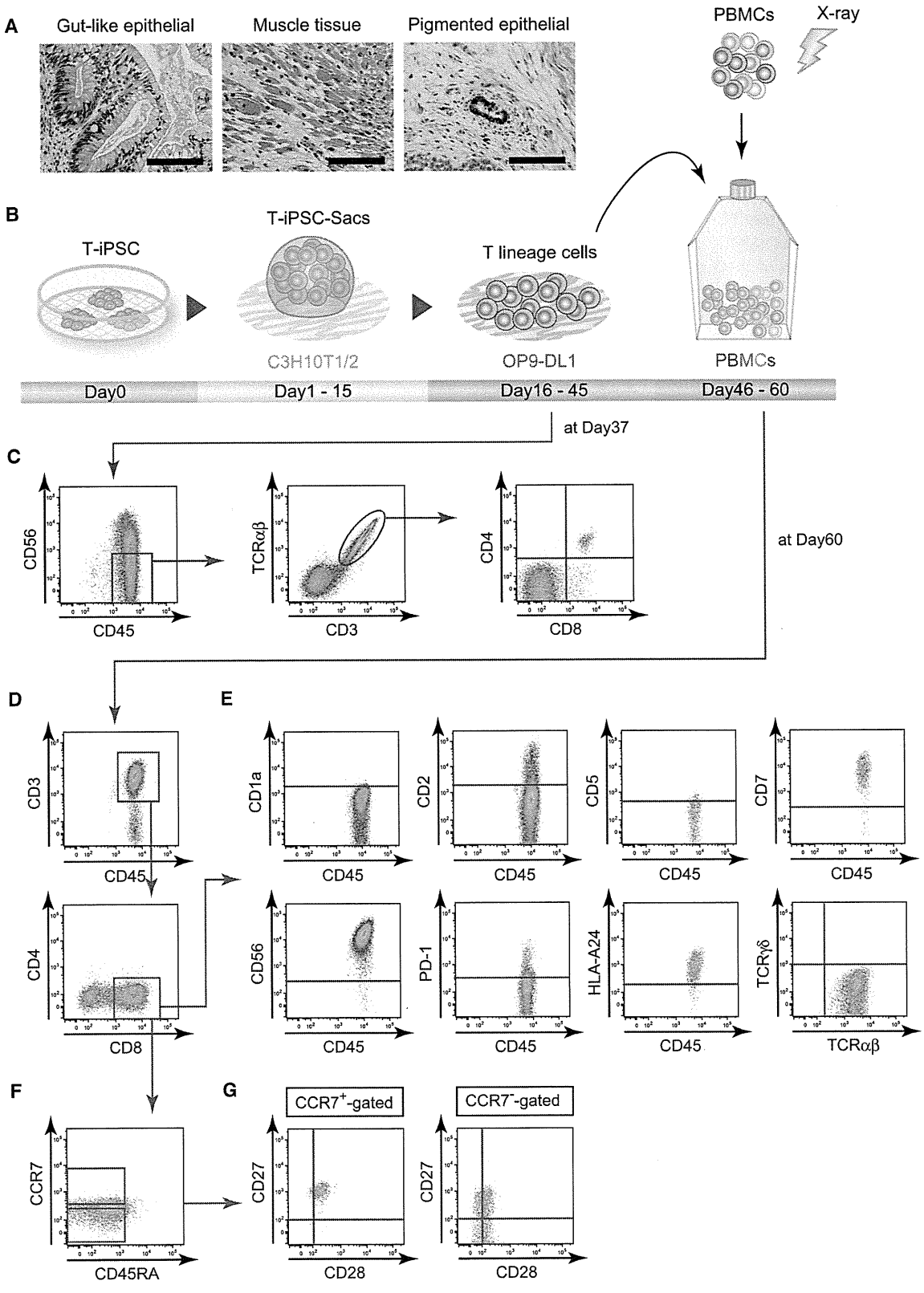

Figure 2. Redifferentiation of T-iPSCs into T Cells

(A) Representative hematoxylin- and eosin-stained sections of a teratoma formed in a NOD/ShiJic-*scid* mouse testis. H254SeVT-3 differentiated into cell lineages derived from endoderm (goblet cells in gut-like epithelial), mesoderm (smooth myocytes in muscle tissue), and ectoderm (retina cells in pigmented epithelial). The scale bar represents 100 μm.

(legend continued on next page)

the T-iPSCs at both the DN and DP stages. By contrast, some *TCRA* mRNAs at the DN and DP stages were identical to those in the T lineage cells, but others differed, and differing sequences were observed more frequently at the DP stage than the DN stage (Table S2). *RAG1* and *RAG2* expression were observed at both the DN and the DP stages, though stronger expression was observed at the DP stage (Figure S5D).

To create mature CD8 SP cells from T-iPSC-derived T lineage cells without receptor revision, we focused on TCR signaling. Turka et al. (1991) reported that TCR signaling via peptide-major histocompatibility complex (MHC) complexes during positive selection ends expression of *RAG* genes and prevents further assembly of TCR genes. They also showed that mimicking TCR signaling using CD3 antibodies had the same effect. Therefore, we tried to stimulate the TCRs of redifferentiating T lineage cells before the completion of the DN-to-DP transition (Figure 2B). For this experiment, we cultured T lineage-committed cells on OP9-DL1, stimulated them with α-CD3/28 beads or PHA (we defined this as the first stimulation) and then cocultured them with irradiated HLA-A24$^-$ PMBCs in the presence of IL-7 and IL-15, which are required for the generation of memory phenotype CD8$^+$ T cells (Kaneko et al., 2009; Prlic et al., 2002; Tan et al., 2002). After 14 days, CD8 SP cells appeared (Figure 2D). These were deemed to be derivatives of H254SeV-3 based on their expression of HLA-A24 (Figure 2E). These CD8 SP cells did not express the immature thymocyte marker CD1a, but they were positive for CD56, which is expressed on CD8$^+$ T cells cultured in vitro (Lu and Negrin, 1994). In addition, these cells expressed CD7 and some CD2, but not CD5. On the one hand, they did not express PD-1, a marker of exhausted T cells (Figure 2E). On the other hand, some of them expressed the memory T cell markers CCR7, CD27, and CD28 simultaneously, thus representing a central memory T cell phenotype (Figures 2F and 2G) (Romero et al., 2007).

To test whether the redifferentiated CD8 SP cells would recognize the same epitope on the same HLA, the entire population of redifferentiated T cells was mixed with the A24/Nef-138-8(WT) tetramer and subjected to flow-cytometric analysis (Kawana-Tachikawa et al., 2002). Most of the CD8 SP cells were stained positively by the A24/Nef-138-8(WT) tetramer, but not by the control tetramer, which represents HIV-1 envelope-derived peptides (RYLRDQQLL; Figure 3A and data not shown). We then collected the A24/Nef-138-8(WT) tetramer-reactive CD8$^+$ cells and expanded them once again using α-CD3/28 beads or PHA stimulation (defined as the second stimulation; Figure 3A). Finally, after several independent redifferentiation experiments, we obtained A24/Nef-138-8(WT) tetramer-reactive CD8 SP cells (reT-1, reT-2.1, reT-2.2, and reT-3). As expected, sequence analysis of *TCRA* and *TCRB* mRNAs in the redifferentiated CD8 SP cells revealed that the TCR gene rearrangement pattern was identical to that in the H25-#4 original T cell clone (Figure 3B and Table 1).

To determine whether the redifferentiated CD8 SP cells were of the T cell lineage, we used quantitative PCR to compare gene-expression profiles among redifferentiated CD8 SP cells, PB CD4$^+$ and CD8$^+$ T cells, and the H25-#4 original T cell clone. As shown in Figure 3C, the expression patterns of CD3, CD4, and CD8 were similar among PB CD8$^+$ T cells, redifferentiated CD8 SP cells, and the H25-#4 original T cell clone. However, the pattern differed from those in PB CD4$^+$ T cells (Figure 3C). Cytotoxic "signature" genes such as granzyme B (*GZMB*), perforin (*PRF1*), interferon-γ (IFN-γ; *IFNG*), and FAS ligand (*FASLG*) were expressed in PB CD8$^+$ T cells. These genes were also expressed relatively strongly in redifferentiated CD8 SP cells and in the H25-#4 original T cell clone; that is, in already-primed T cells (Figure 3D). The expression patterns of several factors involved in transcription or signal transduction and of cell-surface molecules were similar among PB CD8$^+$ T cells, redifferentiated CD8 SP cells, and the H25-#4 original T cell clone (Figure 3E). To exclude the possibility that the redifferentiated CD8 SP cells had acquired natural killer (NK)-like properties during their coculture with OP9-DL1 or PBMCs, we used a complementary DNA (cDNA) microarray to analyze global gene-expression profiles in redifferentiated CD8 cells, the H25-#4 original T cell clone, and PB NK cells. Correlation and cluster analyses of the gene-expression profile of the redifferentiated CD8 SP cells showed it to be similar to that of the H25-#4 original T cell clone but different from that of NK cells (Figures 3F and 3G). These data strongly suggest that T-iPSCs are able to redifferentiate into CD8$^+$ T cells that exhibit the same antigen specificity as that of the original T cell.

Generation of Highly Proliferative T Cells through T-iPSCs

Fewer than 10^5 T lineage cells were obtained from ~3 × 10^5 T-iPSCs after coculture with C3H10T1/2 and OP9-DL1 cells. However, they could be expanded to >10^8 cells with the first stimulation (data not shown). After separating A24/Nef-138-8(WT) tetramer-reactive CD8$^+$ cells, we assessed the expansion rate induced by the second stimulation and also assessed the establishment of reT-1, reT-2.2, and reT-3. We found that these cells expanded from 100-fold to 1,000-fold within 2 weeks in the presence of IL-7 and IL-15, whereas the H25-#4 original T cell clone expanded only about 20-fold (Figure 4A). Even after 100-to-1,000-fold expansions, some cells still expressed central memory T cell markers such as CCR7, CD27, and CD28 (Figure S6). Perhaps with passage through the iPSC state, wherein telomerase activity is quite high (Marion et al., 2009; Takahashi et al., 2007), re-elongation of shortened telomeres in the H25-#4 original T cell clone gives the redifferentiated T cells high replicative potential (Monteiro et al., 1996; Weng et al., 1998). In fact, the redifferentiated T cells carried longer telomeres than the original T cell clone (Figure 4B), an overall process that we call

(B) Schematic illustration of redifferentiation from T-iPSCs into T cells.
(C) Flow-cytometric analysis of the phenotypes of differentiating T lineage cells at 37 days after starting redifferentiation.
(D and E) Flow-cytometric analysis of the phenotypes of T cells at 60 days after starting redifferentiation. Fluorescence-activated cell sorting (FACS) analyses revealed CD8 single-positive maturation (D) and expression of several T cell markers (E).
(F and G) Memory phenotypes of redifferentiated CD8$^+$ T cells. There existed memory-phenotyped cells such as all positive for CCR7 (F), CD27, and CD28 (G). Data are representative of at least three independent experiments. See Figures S3, S4, and S5 and Table S2 for additional data.

Table 2. TCR Gene Rearrangements in H25-4, H254SeVT-3, or Redifferentiated CD8$^+$ T Cells

Cell	Genome or mRNA	Productivity	Rearrangement			Sequence of Junctional Region		
			Vα		Jα	3′Vα	P(N)	5′Jα
TCRA								
H25-4	genome	productive	TRAV8-3*01		TRAJ10*01	TGTGCTGTGGGT	T	TCACGGGAGGAGGAAACAAACTC ACCTTTT
		unproductive[a]	TRAV13-1*01		TRAJ29*01	TGTGCAGCAA	TCC	TCAGGAAACACACCTCTTGTCTTT
H254SeVT-3	genome	productive	TRAV8-3*01		TRAJ10*01	TGTGCTGTGGGT	T	TCACGGGAGGAGGAAACAAACTC ACCTTTT
		unproductive[a]	TRAV13-1*01		TRAJ29*01	TGTGCAGCAA	TCC	TCAGGAAACACACCTCTTGTCTTT
reT-1	mRNA	productive	TRAV8-3*01		TRAJ10*01	TGTGCTGTGGGT	T	TCACGGGAGGAGGAAACAAACTC ACCTTTT
		unproductive[a]	TRAV13-1*01		TRAJ29*01	TGTGCAGCAA	TCC	TCAGGAAACACACCTCTTGTCTTT
reT-2.1	mRNA	productive	TRAV8-3*01		TRAJ10*01	TGTGCTGTGGGT	T	TCACGGGAGGAGGAAACAAACTC ACCTTTT
		unproductive[a]	TRAV13-1*01		TRAJ29*01	TGTGCAGCAA	TCC	TCAGGAAACACACCTCTTGTCTTT
reT-3	mRNA	productive	TRAV8-3*01		TRAJ10*01	TGTGCTGTGGGT	T	TCACGGGAGGAGGAAACAAACTC ACCTTTT
		unproductive[a]	TRAV13-1*01		TRAJ29*01	TGTGCAGCAA	TCC	TCAGGAAACACACCTCTTGTCTTT
			Vβ	Dβ	Jβ	3′Vβ	N1-Dβ-N2	5′Jβ
TCRB								
H25-4	genome	productive	TRBV7-9*01	TRBD1*01	TRBJ2-5*01	TGTGCCAGCAGCTTA	CGGGACAGGGTGCCG	GAGACCCAGTACTTC
		unproductive	germline	TRBD1*01	TRBJ2-7*01	TACAAAGCTGTAACATTGTG	GGGACAACT	CTACGAGCAGTACTTCGGGCCG
H254SeVT-3	genome	productive	TRBV7-9*01	TRBD1*01	TRBJ2-5*01	TGTGCCAGCAGCTTA	CGGGACAGGGTGCCG	GAGACCCAGTACTTC
		unproductive	germline	TRBD1*01	TRBJ2-7*01	TACAAAGCTGTAACATTGTG	GGGACAACT	CTACGAGCAGTACTTCGGGCCG
reT-1	mRNA	productive	TRBV7-9*01	TRBD1*01	TRBJ2-5*01	TGTGCCAGCAGCTTA	CGGGACAGGGTGCCG	GAGACCCAGTACTTC
reT-2.1	mRNA	productive	TRBV7-9*01	TRBD1*01	TRBJ2-5*01	TGTGCCAGCAGCTTA	CGGGACAGGGTGCCG	GAGACCCAGTACTTC
reT-3	mRNA	productive	TRBV7-9*01	TRBD1*01	TRBJ2-5*01	TGTGCCAGCAGCTTA	CGGGACAGGGTGCCG	GAGACCCAGTACTTC

PCR-amplified samples (H25-4: not shown; H254SeVT-3: shown in Figures 1J and 1K; reT-1, reT-2.1, and reT-3: shown in Figure 3B) were sequenced, then V, D, and J segment usages and junctional sequences in CDR3 were identified. Following reprogramming and redifferentiation, there were no alterations in gene rearrangement in either allele at the *TCRA* and *TCRB* gene loci. See Table S1 for additional data on another T-iPSC clone (TkT3V1-7).

[a]Out-of-frame junction (at CDR3).

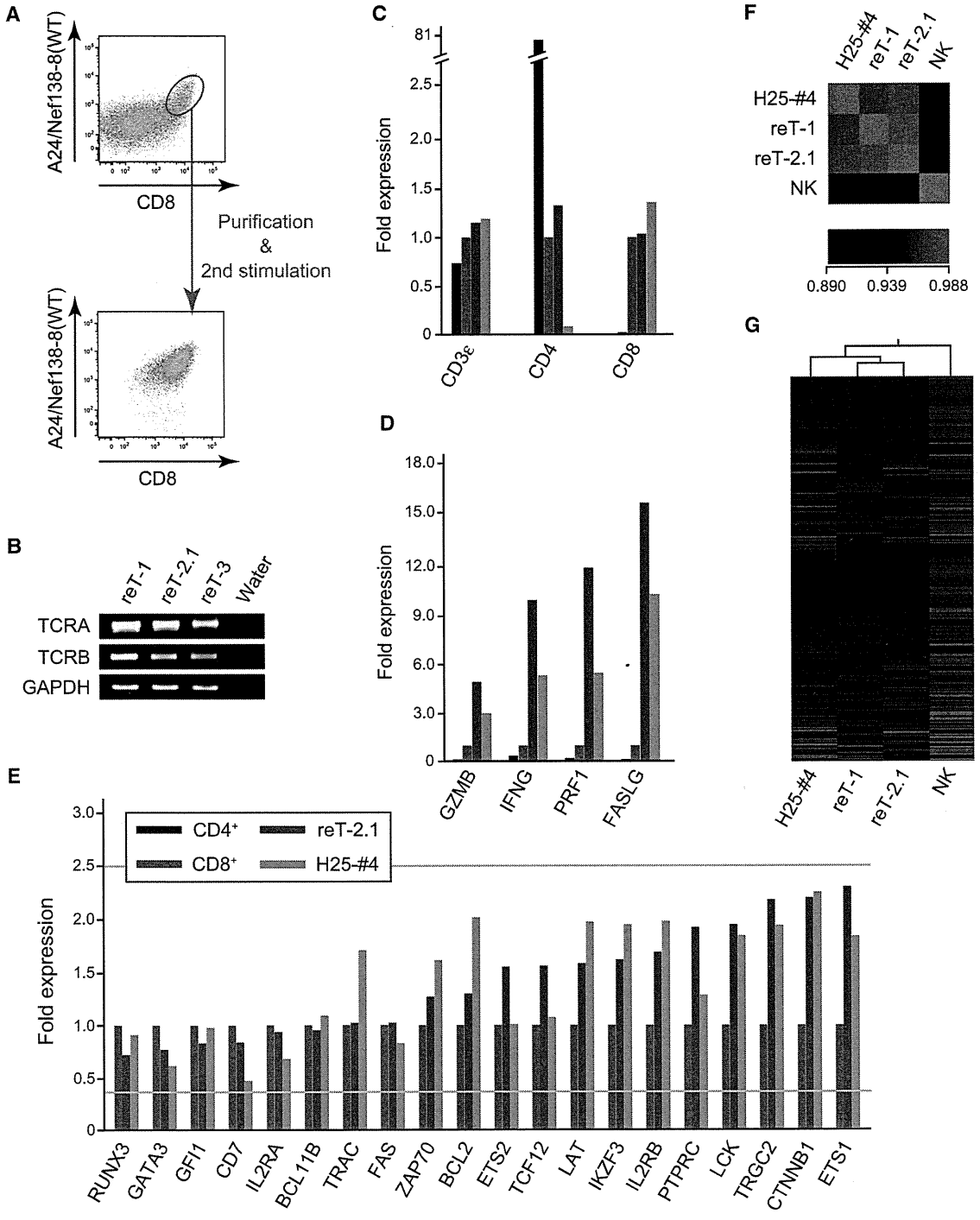

Figure 3. Characterizations of Redifferentiated T Cells as T Cells

(A) Recognition of A24/Nef-138-8(WT) tetramer at 50–60 days after starting redifferentiation, analyzed by flow cytometry (upper panel). Tetramer-positive cells were sorted by FACS or magnetically selected, then cultured for an additional 14 days, after which the expanded T cells were reanalyzed for tetramer (lower panel).

(B) TCR mRNAs were identified in a SMART-mediated cDNA library for reT-1, reT-2.1, and reT-3 cells. *GAPDH* is an internal control for PCRs.

(C–E) Quantitative PCR to compare the expression of major cell surface molecules (C), cell lytic molecules (D), and transcription factors and signal-transduction molecules (E) among PB $CD4^+$, PB $CD8^+$, reT-2.1, and H25-#4 cells. Individual PCR reactions were normalized against 18S rRNA.

(F and G) Global gene expression was analyzed using a cDNA microarray. Heat maps show the correlation coefficients between samples (F) and differential expression (>3-fold) of genes relative to NK cells (G). Red and green colorations indicate increased and decreased expression, respectively.

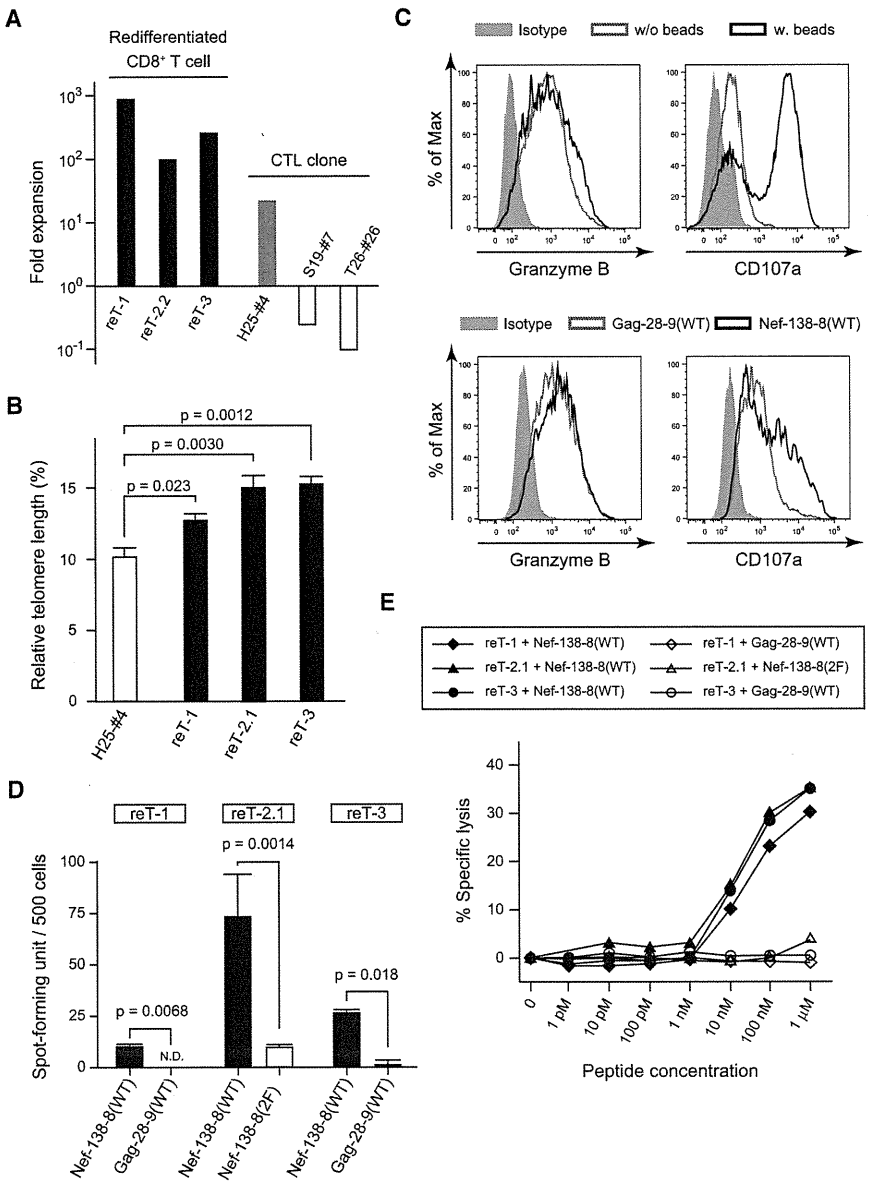

Figure 4. Redifferentiated T Cells Show T Cell Functionality and the Same Antigen Specificity as the Original CTL Clone

(A) Expansion ratios for reT-1, reT-2.2, and reT-3 cells elicited by PHA, IL-7, and IL-15 stimulation for 2 weeks. H25-#4 is the original clone. S19-#7 and T26-#26 were other Nef-138-8(WT)-specific CTL clones derived from different patients.

(B) Relative telomere length determined using flow-FISH. Data are presented as mean ± SEM.

(C) Intracellular production of granzyme B (left panel) and CD107a mobilization (right panel) induced by stimulation of reT-2.1 cells with α-CD3/CD28 beads or Nef-138-8(WT). Shaded plot: stimulated cells, isotype antibody; gray line: unstimulated cells, granzyme B or CD107a antibody; black line: stimulated cells, granzyme B or CD107a antibody.

(D) IFN-γ production in the presence of Nef-138-8(WT) measured using ELISPOT. Data are presented as mean ± SD. N.D., not determined.

(E) Standard ^{51}Cr release assay performed using the indicated concentrations of Nef-138-8(WT). Effector:target = 5:1.

See Figure S6 for additional data.

"rejuvenation." Throughout the experiments, neither autonomous cell expansion nor aberrant cell survival without cytokines as leukemia cells was observed (data not shown). Taken together, these data indicate that by passing through the T-iPSC state, cloned cytotoxic T cells can become "rejuvenated" to central memory-like T cells with excellent potential for proliferation and survival.

Redifferentiated CD8$^+$ T Cells Exhibit Antigen-Specific T Cell Functionality

To determine whether redifferentiated CD8$^+$ T cells exerted cytotoxic effects upon recognition of specific peptides in the context of an MHC, we performed functional assays using HLA-A24-positive B-LCL cells as antigen-presenting cells. Gag-28-9(WT) (KYKLKHIVW) is an antigenic peptide (aa 28–36) from the HIV-1 Gag protein (Altfeld et al., 2006), whereas Nef-138-8(2F) (RFPLTFGW) is a Tyr-to-Phe-substituted single-residue mutant form of Nef-138-8(WT). Both peptides were presented on HLA-A24 cells.

One of the major mechanisms by which CTLs induce cytotoxity is the secretion of cytolytic molecules triggered by TCR signaling. Intracellular staining revealed that the cytolytic molecule granzyme B was produced and stored in the granules of redifferentiated CD8$^+$ T cells (Figure 4C, left column). CD107a, also known as lysosomal-associated membrane protein 1 (LAMP1), is a granulocyte membrane protein that transiently appears at the cell surface and is coupled to degranulation (secretion of cytolytic molecules) of the stimulated CTLs, after which CD107a returns to the cytoplasm (Rubio et al., 2003). CD107a molecules on the cell surface were captured by a fluorochrome-conjugated antibody when redifferentiated CD8$^+$ T cells were stimulated with α-CD3/28 beads or Nef-138-8(WT) peptide, but not in the absence of the beads or Gag-28-9(WT) peptide (Figure 4C, right column). In the second experiment, we used the enzyme-linked immunosorbent spot (ELISPOT) assay to assess cytokine productivity per cell and confirmed that redifferentiated CD8$^+$ T cells produced significant levels of IFN-γ in response to stimulation by its specific antigen, Nef-138-8(WT) (Figure 4D). In a separate experiment, we used a ^{51}Cr release assay to investigate cytolytic capacity and found that redifferentiated CD8$^+$ T cells lysed ^{51}Cr-incorporated B-LCLs only when Nef-138-8(WT) was presented on B-LCLs (Figure 4E).

These results are highly indicative that redifferentiated CD8$^+$ T cells can release cytotoxic molecules and kill antigen-expressing target cells in an antigen-specific manner. Moreover,

monoclonal TCRs mediate highly precise cell targeting that should broaden the therapeutic window for antigen-specific T cell therapy by avoiding the troublesome mispairing TCRs that can occur with the commonly used exogenous TCR transfer technique for inducing antigen-specific T cells from hematopoietic stem cells or peripheral mature T cells (Bendle et al., 2010; Brenner and Okur, 2009).

DISCUSSION

Using a HIV-1-epitope-specific CTL clone as a model, we demonstrated here that the reprogramming into pluripotency of a T cell clone and the subsequent redifferentiation to mature functional $CD8^+$ T cells are possible. These redifferentiated $CD8^+$ T cells are highly proliferative naive cells with elongated telomeres, and they exert T cell functions in the same HIV-1-epitope-specific manner, permitting the inference that this process of reprogramming and redifferentiation can rejuvenate mature antigen-specific T cells.

Generation of iPSCs from T cells was initially difficult. On the basis of reports by Seki et al. (2010), we also found that SeV is suitable for the reprogramming of aged and exhausted fibroblasts, as well as of T cells. We also found that coexpression of SV40 large T antigen acted synergistically with the classic Yamanaka factors in enhancing the reprogramming efficiency of T cells. Therefore, SV40 large-T antigen introduction using the SeV vector system was also included in the protocol. Worth noting is that c-*MYC* is a known oncogene, and when it is inserted into the genomic DNA by the retroviral vector, it may become a risk for tumorigenesis in the generation of iPSCs. The same concern does not apply to SeV vector systems, given that the genomic RNA could be removed from the cytosol after reprogramming. Therefore, the utilization of SeV vectors both improved reprogramming efficiency and shielded redifferentiating cells from oncogene- or provirus-mediated tumorigenesis (Kohn et al., 2003).

In the redifferentiation experiments, mimicking TCR signaling led to CD8-linage specification without reassembly of *TCRA* genes. Preassembled TCR genes are a distinctive feature of T-iPSCs not found on other pluripotent stem cells. TCR$\alpha\beta$ is aberrantly expressed on redifferentiating CD4/CD8 DN cells, and the TCR signaling evoked results in the cessation of *RAG* expression. Serwold and colleagues reported that aberrantly early expression of TCR from preassembled *Tcra* and *Tcrb* following TCR signaling in murine thymocytes drives later lymphomagenesis (Serwold et al., 2010). They cautioned that T-iPSCs might confer risk for TCR-mediated lymphomagenesis. Therefore, the redifferentiation method will need to be further optimized and confirmed for clinical safety before application in practical treatments. This may be achieved by the use of an inducible suicide-gene system for eliminating unwanted tumors after injections (Hara et al., 2008; Veldwijk et al., 2004).

Immunological assays found that the redifferentiated $CD8^+$ T cells exerted T cell functions such as cytolytic activity, IFN-γ secretion, and degranulation in a normal manner when stimulated with their specific antigens. The most striking difference was in their proliferation capacity and elongated telomeres, which correlates with the central-memory T cell phenotype. Stem cell-like memory T cells (T_{SCM}) were recently identified as a subpopulation of T cells that has the capacity for self-renewal and that is multipotent and able to generate central memory, effector memory, and effector T cells (Gattinoni et al., 2011; Turtle et al., 2009). In a humanized mouse model, T_{SCM} cells reconstituted the T cell population more efficiently than other known memory subsets while mediating a superior antitumor response. It was found that inhibition of GSK3β enhances the generation of T_{SCM} in culture. Combining T-iPSC-mediated T cell rejuvenation with GSK3β inhibition may therefore enable efficient generation of T_{SCM} cells and permit highly effective immunotherapy along with the reconstitution of a normal T cell immune system.

Although these data suggest that rejuvenated T cells enjoy an advantage over the original T cell clone, it remains unclear whether these HIV-epitope-specific rejuvenated T cells are effective in improving the overall status of HIV infection. This is because the role of $CD8^+$ T cells in HIV infection appears to vary depending on the disease stage (Appay et al., 2000; Borrow et al., 1994; Brodie et al., 1999; Day et al., 2006; Koup et al., 1994). Evasion of the immune response through CTL escape is another important factor in HIV pathogenesis, and the escaped virus is a substantial hurdle for HIV therapies (Phillips et al., 1991). Therefore, this system may work best instead against tumors such as a melanoma, for which certain antigenic epitopes are known, or against viral infections other than HIV, for which the roles of $CD8^+$ cytotoxic T cells are more established. Nonetheless, the system described in our study will make it possible to preserve and to supply highly proliferative, functional $CD8^+$ T cells specific to a variety of HIV epitopes without worrying about exhaustion. It may also act as a valuable tool in better understanding the role of adoptive immunity in HIV infection.

Here, we have presented a proof of concept of $CD8^+$ T cell rejuvenation. The concept is not limited only to $CD8^+$ cytotoxic T cells. It may also be applied to $CD4^+$ helper or regulatory T cells to control desired or undesired immune reactions in the context of malignancies, chronic viral infections, autoimmune diseases, or transplantation-related immune disorders, if optimization of redifferentiation conditions can be achieved. Biological and technical challenges lie ahead, but the data presented in this work open new avenues toward antigen-specific T cell therapies that will supply unlimited numbers of rejuvenated T cells and will regenerate patients' immune systems.

EXPERIMENTAL PROCEDURES

Generation of Antigen-Specific CTL Clones

Nef138-8(WT)-specific CTL lines were induced from PBMCs of a patient chronically infected with HIV-1 who is positive for HLA-A24, as described (Kawana-Tachikawa et al., 2002). Each CTL line was expanded from a single-cell sorted $tetramer^+$ T cell, and the cells in every CTL line were confirmed for expression of only one kind of TCR$\alpha\beta$. For more details of CTL-clone establishment, see the Supplemental Experimental Procedures.

Generation of T-iPSCs

Human iPSCs were established from PB T cells or a CTL clone as described (Takayama et al., 2010), slightly modifying the culture conditions. In brief, T cells were stimulated by α-CD3/CD28 antibody-coated beads (Miltenyi Biotec) or by 5 μg/ml PHA-L (Sigma-Aldrich). The activated cells were transduced with reprogramming factors via retroviral or SeV vectors and were cultured in RH10 medium (RPMI-1640 supplemented with 10% human AB Serum, 2 mM L-glutamine, 100 U/ml penicillin, and 100 ng/ml streptomycin), which was

gradually replaced with human iPSC medium (Dulbecco's modified Eagle's medium/F12 FAM supplemented with 20% knockout serum replacer, 2 mM L-glutamine, 1% nonessential amino acids, 10 μM 2-mercaptoethanol, and 5 ng/ml basic fibroblast growth factor [bFGF]). The established iPSC clones were transfected with small interfering RNA L527 (Nishimura et al., 2011) using Lipofectamine RNAi Max (Invitrogen) for removal of SeV vectors from the cytoplasm.

Analysis of TCR Gene Rearrangement in Genomic DNA

Genomic DNA was extracted from approximately 5 × 10^6 cells using QIAamp DNA kits (QIAGEN) according to the manufacturer's instructions. For *TCRB* gene rearrangement analysis, PCR was performed according to BIOMED-2 protocols (van Dongen et al., 2003). For *TCRA* gene rearrangement analysis, PCR was performed using the primers shown in Figure S2 and LA Taq HS (TaKaRa). The PCR protocol entailed three amplification cycles (30 s at 95°C, 45 s at 68°C, and 6 min at 72°C); 15 amplification cycles (30 s at 95°C, 45 s at 62°C, and 6 min at 72°C); and 12 amplification cycles (15 s at 95°C, 30 s at 62°C, and 6 min at 72°C). The dominant band within the expected size range was purified using a QIAquick gel-extraction kit (QIAGEN) and was then sequenced. V, D, and J segment usages were identified by comparison to the ImMunoGeneTics (IMGT) database (http://www.imgt.org/) and by using an online tool (IMGT/V-QUEST) (Lefranc, 2003). Gene-segment nomenclature follows IMGT usage.

Analysis of TCR Gene Rearrangement in mRNA

A method based on the "switch mechanism at the 5′-end of the reverse transcript (SMART)" (Du et al., 2006) was used to synthesize double-stranded cDNAs (Super SMART cDNA synthesis kit; BD Clontech). Reverse transcription was conducted with the 3′ SMART CDS primer, SMART II A oligonucleotides (Super SMART cDNA synthesis kit), and PrimeScript Reverse Transcriptase (TaKaRa) for 90 min at 42°C. Double-stranded cDNA was then synthesized and was amplified with 5′ PCR Primer II A (Super SMART cDNA synthesis kit), and reagents were provided in an Advantage 2 PCR Kit (BD Clontech). The PCR protocol entailed 20 cycles of 5 s at 95°C, 5 s at 65°C, and 3 min at 68°C. The amplified double-stranded cDNA was used as templates in TCRA- or TCRB-specific amplification reactions. With forward primer (2^{nd}_5′-SMART) and reverse primer (3′-TRAC for *TCRA* or 3′-TRBC for *TCRB*), 25 cycles of amplification were performed (30 s at 94°C, 30 s at 55°C, and 1 min at 72°C). PCR products were cloned into pGEM-T Easy Vector (Promega) and were sequenced.

T Cell Differentiation from T-iPSCs

To differentiate human iPSCs into hematopoietic cells, we slightly modified a previously described protocol (Takayama et al., 2008). Small clumps of iPSCs (<100 cells) were transferred onto irradiated C3H10T1/2 cells and co-cultured in EB medium (Iscove's modified Dulbecco's medium supplemented with 15% fetal bovine serum [FBS] and a cocktail of 10 μg/ml human insulin, 5.5 μg/ml human transferrin, 5 ng/ml sodium selenite, 2 mM L-glutamine, 0.45 mM α-monothioglycerol, and 50 μg/ml ascorbic acid) in the presence of VEGF, SCF, and FLT-3L. Hematopoietic cells contained in iPSC sacs were collected and were transferred onto irradiated OP9-DL1 cells (provided by RIKEN BRC through the National BioResource Project of the Ministry of Education, Culture, Sports, Science, and Technology [MEXT]) (Watarai et al., 2010). The hematopoietic cells underwent T lineage differentiation on OP9-DL1 cells during coculture in OP9 medium (αMEM supplemented with 15% FBS, 2 mM L-glutamine, 100 U/ml penicillin, and 100 ng/ml streptomycin) in the presence of FLT-3L and IL-7. The T lineage cells were then harvested, mixed with irradiated HLA-A24$^-$ PBMCs, and cocultured in RH10 medium in the presence of IL-7 and IL-15.

Intracellular Staining

For intracellular staining of granzyme B, T cells were stimulated by α-CD3/28 beads or peptide-loaded HLA-A24$^+$ B-LCLs. After 2 hr, brefeldin A (5 μg/ml; Invitrogen) was added, with incubation for 4 hours more. Cells were then harvested and fixed in Fixation/Permeabilization solution (BD Biosciences). Intracellular staining was performed as per the manufacturer's protocol using Perm/Wash buffer (BD Biosciences) and fluorescein isothiocyanate (FITC)-conjugated granzyme B antibody (BD Biosciences). For capturing CD107a transiently expressed on cell surfaces, T cells were incubated with α-CD3/28 beads or peptide-loaded HLA-A24$^+$ B-LCLs and were cultured with FITC-conjugated CD107a antibody (BioLegend) for 6 hr. Harvested cells were fixed and stained as described above. Data were acquired on FACSAria II equipment (BD Biosciences) and analyzed using FlowJo software (Tree Star).

Measurement of Telomere Length by Flow-FISH

Telomere length was measured using a Telomere PNA Kit/FITC (DAKO) as previously described (Neuber et al., 2003).

ELISPOT and ^{51}Cr Release Assays

The antigen-specific responses of T cells were measured using an ELISPOT assay for IFN-γ and a standard ^{51}Cr release assay as described (Kawana-Tachikawa et al., 2002; Tsunetsugu-Yokota et al., 2003). HLA-A24$^+$ B-LCLs were used as antigen-presenting cells.

Statistics

All data are presented as mean ± SD. All statistics were performed using Excel (Microsoft) and Prism (GraphPad software) programs, applying two-tailed Student's t test. Values of $p < 0.05$ were considered significant. For additional details, see the Supplemental Experimental Procedures.

ACCESSION NUMBERS

The Gene Expression Omnibus accession number for microarray data reported in this paper is GSE43136.

SUPPLEMENTAL INFORMATION

Supplemental Information includes six figures, three tables, and Supplemental Experimental Procedures and can be found with this article online at http://dx.doi.org/10.1016/j.stem.2012.11.002.

ACKNOWLEDGMENTS

We thank Yumiko Ishii and Yuji Yamazaki (The University of Tokyo) for FACS operation; Sou Nakamura, Ryoko Jono-Onishi, and Shuichi Kitayama (The University of Tokyo) for technical help; Hiroshi Kawamoto, Kyoko Masuda, and Raul Vizcardo (RIKEN Center for Allergy and Immunology) for kindly providing OP9-DL1 cells and for helpful discussions; Yasuharu Nishimura and Satoru Senju (Kumamoto University) for kindly providing T cell clones; Makoto Otsu, Akihide Kamiya, Motoo Watanabe, Ayako Kamisato, and Masataka Kasai (The University of Tokyo) and Masaki Yasukawa, Hiroshi Fujiwara, and Toshiki Ochi (Ehime University) for helpful discussions; and Alex Knisely and Huan-Ting Lin for critical reading of the manuscript. The project was supported in part by a grant from the Project for Realization of Regenerative Medicine, by a Grant-in-Aid for Scientific Research (KAKENHI) and by the Global Center of Excellence program from MEXT of Japan, by a Grant-in-Aid for scientific research from the Japan Society for the Promotion of Science, and by grants for AIDS research from the Ministry of Health, Labor, and Welfare of Japan. The experimental protocol was approved by the institutional regulation board for human ethics at the Institute of Medical Science, University of Tokyo (approval number: 20-6-0826). The entire study was conducted in accordance with the Declaration of Helsinki.

Received: May 31, 2012
Revised: September 28, 2012
Accepted: November 6, 2012
Published: January 3, 2013

REFERENCES

Alt, F.W., and Baltimore, D. (1982). Joining of immunoglobulin heavy chain gene segments: implications from a chromosome with evidence of three D-JH fusions. Proc. Natl. Acad. Sci. USA *79*, 4118–4122.

Altfeld, M., Kalife, E.T., Qi, Y., Streeck, H., Lichterfeld, M., Johnston, M.N., Burgett, N., Swartz, M.E., Yang, A., Alter, G., et al. (2006). HLA Alleles

Associated with Delayed Progression to AIDS Contribute Strongly to the Initial CD8(+) T Cell Response against HIV-1. PLoS Med. *3*, e403.

Appay, V., Nixon, D.F., Donahoe, S.M., Gillespie, G.M., Dong, T., King, A., Ogg, G.S., Spiegel, H.M., Conlon, C., Spina, C.A., et al. (2000). HIV-specific CD8(+) T cells produce antiviral cytokines but are impaired in cytolytic function. J. Exp. Med. *192*, 63–75.

Bendle, G.M., Linnemann, C., Hooijkaas, A.I., Bies, L., de Witte, M.A., Jorritsma, A., Kaiser, A.D., Pouw, N., Debets, R., Kieback, E., et al. (2010). Lethal graft-versus-host disease in mouse models of T cell receptor gene therapy. Nat. Med. *16*, 565–570, 1p following 570.

Borgulya, P., Kishi, H., Uematsu, Y., and von Boehmer, H. (1992). Exclusion and inclusion of alpha and beta T cell receptor alleles. Cell *69*, 529–537.

Borrow, P., Lewicki, H., Hahn, B.H., Shaw, G.M., and Oldstone, M.B. (1994). Virus-specific CD8+ cytotoxic T-lymphocyte activity associated with control of viremia in primary human immunodeficiency virus type 1 infection. J. Virol. *68*, 6103–6110.

Brenner, M.K., and Okur, F.V. (2009). Overview of gene therapy clinical progress including cancer treatment with gene-modified T cells. Hematology (Am. Soc. Hematol. Educ. Program), 675–681.

Brivanlou, A.H., Gage, F.H., Jaenisch, R., Jessell, T., Melton, D., and Rossant, J. (2003). Stem cells. Setting standards for human embryonic stem cells. Science *300*, 913–916.

Brodie, S.J., Lewinsohn, D.A., Patterson, B.K., Jiyamapa, D., Krieger, J., Corey, L., Greenberg, P.D., and Riddell, S.R. (1999). In vivo migration and function of transferred HIV-1-specific cytotoxic T cells. Nat. Med. *5*, 34–41.

Brown, M.E., Rondon, E., Rajesh, D., Mack, A., Lewis, R., Feng, X., Zitur, L.J., Learish, R.D., and Nuwaysir, E.F. (2010). Derivation of induced pluripotent stem cells from human peripheral blood T lymphocytes. PLoS ONE *5*, e11373.

Butler, N.S., Nolz, J.C., and Harty, J.T. (2011). Immunologic considerations for generating memory CD8 T cells through vaccination. Cell. Microbiol. *13*, 925–933.

Day, C.L., Kaufmann, D.E., Kiepiela, P., Brown, J.A., Moodley, E.S., Reddy, S., Mackey, E.W., Miller, J.D., Leslie, A.J., DePierres, C., et al. (2006). PD-1 expression on HIV-specific T cells is associated with T-cell exhaustion and disease progression. Nature *443*, 350–354.

Du, G., Qiu, L., Shen, L., Sehgal, P., Shen, Y., Huang, D., Letvin, N.L., and Chen, Z.W. (2006). Combined megaplex TCR isolation and SMART-based real-time quantitation methods for quantitating antigen-specific T cell clones in mycobacterial infection. J. Immunol. Methods *308*, 19–35.

Freberg, C.T., Dahl, J.A., Timoskainen, S., and Collas, P. (2007). Epigenetic reprogramming of OCT4 and NANOG regulatory regions by embryonal carcinoma cell extract. Mol. Biol. Cell *18*, 1543–1553.

Fusaki, N., Ban, H., Nishiyama, A., Saeki, K., and Hasegawa, M. (2009). Efficient induction of transgene-free human pluripotent stem cells using a vector based on Sendai virus, an RNA virus that does not integrate into the host genome. Proc. Jpn. Acad., Ser. B, Phys. Biol. Sci. *85*, 348–362.

Gattinoni, L., Lugli, E., Ji, Y., Pos, Z., Paulos, C.M., Quigley, M.F., Almeida, J.R., Gostick, E., Yu, Z., Carpenito, C., et al. (2011). A human memory T cell subset with stem cell-like properties. Nat. Med. *17*, 1290–1297.

Greenberg, P.D. (1991). Adoptive T cell therapy of tumors: mechanisms operative in the recognition and elimination of tumor cells. Adv. Immunol. *49*, 281–355.

Hanna, J., Markoulaki, S., Schorderet, P., Carey, B.W., Beard, C., Wernig, M., Creyghton, M.P., Steine, E.J., Cassady, J.P., Foreman, R., et al. (2008). Direct reprogramming of terminally differentiated mature B lymphocytes to pluripotency. Cell *133*, 250–264.

Hara, A., Aoki, H., Taguchi, A., Niwa, M., Yamada, Y., Kunisada, T., and Mori, H. (2008). Neuron-like differentiation and selective ablation of undifferentiated embryonic stem cells containing suicide gene with Oct-4 promoter. Stem Cells Dev. *17*, 619–627.

Hochedlinger, K., and Jaenisch, R. (2002). Monoclonal mice generated by nuclear transfer from mature B and T donor cells. Nature *415*, 1035–1038.

Huang, C., and Kanagawa, O. (2001). Ordered and coordinated rearrangement of the TCR alpha locus: role of secondary rearrangement in thymic selection. J. Immunol. *166*, 2597–2601.

Ikawa, T., Hirose, S., Masuda, K., Kakugawa, K., Satoh, R., Shibano-Satoh, A., Kominami, R., Katsura, Y., and Kawamoto, H. (2010). An essential developmental checkpoint for production of the T cell lineage. Science *329*, 93–96.

Jameson, S.C., and Masopust, D. (2009). Diversity in T cell memory: an embarrassment of riches. Immunity *31*, 859–871.

June, C.H. (2007). Adoptive T cell therapy for cancer in the clinic. J. Clin. Invest. *117*, 1466–1476.

Kaneko, S., Mastaglio, S., Bondanza, A., Ponzoni, M., Sanvito, F., Aldrighetti, L., Radrizzani, M., La Seta-Catamancio, S., Provasi, E., Mondino, A., et al. (2009). IL-7 and IL-15 allow the generation of suicide gene-modified alloreactive self-renewing central memory human T lymphocytes. Blood *113*, 1006–1015.

Kawana-Tachikawa, A., Tomizawa, M., Nunoya, J., Shioda, T., Kato, A., Nakayama, E.E., Nakamura, T., Nagai, Y., and Iwamoto, A. (2002). An efficient and versatile mammalian viral vector system for major histocompatibility complex class I/peptide complexes. J. Virol. *76*, 11982–11988.

Khor, B., and Sleckman, B.P. (2002). Allelic exclusion at the TCRbeta locus. Curr. Opin. Immunol. *14*, 230–234.

Klebanoff, C.A., Gattinoni, L., and Restifo, N.P. (2006). CD8+ T-cell memory in tumor immunology and immunotherapy. Immunol. Rev. *211*, 214–224.

Kohn, D.B., Sadelain, M., and Glorioso, J.C. (2003). Occurrence of leukaemia following gene therapy of X-linked SCID. Nat. Rev. Cancer *3*, 477–488.

Koup, R.A., Safrit, J.T., Cao, Y., Andrews, C.A., McLeod, G., Borkowsky, W., Farthing, C., and Ho, D.D. (1994). Temporal association of cellular immune responses with the initial control of viremia in primary human immunodeficiency virus type 1 syndrome. J. Virol. *68*, 4650–4655.

Krangel, M.S. (2009). Mechanics of T cell receptor gene rearrangement. Curr. Opin. Immunol. *21*, 133–139.

Lafaille, J.J., DeCloux, A., Bonneville, M., Takagaki, Y., and Tonegawa, S. (1989). Junctional sequences of T cell receptor gamma delta genes: implications for gamma delta T cell lineages and for a novel intermediate of V-(D)-J joining. Cell *59*, 859–870.

Lefranc, M.P. (2003). IMGT databases, web resources and tools for immunoglobulin and T cell receptor sequence analysis, http://imgt.cines.fr. Leukemia *17*, 260–266.

Loh, Y.H., Hartung, O., Li, H., Guo, C., Sahalie, J.M., Manos, P.D., Urbach, A., Heffner, G.C., Grskovic, M., Vigneault, F., et al. (2010). Reprogramming of T cells from human peripheral blood. Cell Stem Cell *7*, 15–19.

Lu, P.H., and Negrin, R.S. (1994). A novel population of expanded human CD3+CD56+ cells derived from T cells with potent in vivo antitumor activity in mice with severe combined immunodeficiency. J. Immunol. *153*, 1687–1696.

MacLeod, M.K., Kappler, J.W., and Marrack, P. (2010). Memory CD4 T cells: generation, reactivation and re-assignment. Immunology *130*, 10–15.

Marion, R.M., Strati, K., Li, H., Tejera, A., Schoeftner, S., Ortega, S., Serrano, M., and Blasco, M.A. (2009). Telomeres acquire embryonic stem cell characteristics in induced pluripotent stem cells. Cell Stem Cell *4*, 141–154.

Monteiro, J., Batliwalla, F., Ostrer, H., and Gregersen, P.K. (1996). Shortened telomeres in clonally expanded CD28-CD8+ T cells imply a replicative history that is distinct from their CD28+CD8+ counterparts. J. Immunol. *156*, 3587–3590.

Morgan, R.A., Dudley, M.E., Wunderlich, J.R., Hughes, M.S., Yang, J.C., Sherry, R.M., Royal, R.E., Topalian, S.L., Kammula, U.S., Restifo, N.P., et al. (2006). Cancer regression in patients after transfer of genetically engineered lymphocytes. Science *314*, 126–129.

Neuber, K., Schmidt, S., and Mensch, A. (2003). Telomere length measurement and determination of immunosenescence-related markers (CD28, CD45RO, CD45RA, interferon-gamma and interleukin-4) in skin-homing T cells expressing the cutaneous lymphocyte antigen: indication of a non-ageing T-cell subset. Immunology *109*, 24–31.

Nishimura, K., Sano, M., Ohtaka, M., Furuta, B., Umemura, Y., Nakajima, Y., Ikehara, Y., Kobayashi, T., Segawa, H., Takayasu, S., et al. (2011). Development of defective and persistent Sendai virus vector: a unique gene delivery/expression system ideal for cell reprogramming. J. Biol. Chem. *286*, 4760–4771.

Padovan, E., Casorati, G., Dellabona, P., Meyer, S., Brockhaus, M., and Lanzavecchia, A. (1993). Expression of two T cell receptor alpha chains: dual receptor T cells. Science *262*, 422–424.

Petrie, H.T., Livak, F., Schatz, D.G., Strasser, A., Crispe, I.N., and Shortman, K. (1993). Multiple rearrangements in T cell receptor alpha chain genes maximize the production of useful thymocytes. J. Exp. Med. *178*, 615–622.

Phillips, R.E., Rowland-Jones, S., Nixon, D.F., Gotch, F.M., Edwards, J.P., Ogunlesi, A.O., Elvin, J.G., Rothbard, J.A., Bangham, C.R., Rizza, C.R., et al. (1991). Human immunodeficiency virus genetic variation that can escape cytotoxic T cell recognition. Nature *354*, 453–459.

Porter, D.L., Levine, B.L., Kalos, M., Bagg, A., and June, C.H. (2011). Chimeric antigen receptor-modified T cells in chronic lymphoid leukemia. N. Engl. J. Med. *365*, 725–733.

Prlic, M., Lefrancois, L., and Jameson, S.C. (2002). Multiple choices: regulation of memory CD8 T cell generation and homeostasis by interleukin (IL)-7 and IL-15. J. Exp. Med. *195*, F49–F52.

Romero, P., Zippelius, A., Kurth, I., Pittet, M.J., Touvrey, C., Iancu, E.M., Corthesy, P., Devevre, E., Speiser, D.E., and Rufer, N. (2007). Four functionally distinct populations of human effector-memory CD8+ T lymphocytes. J. Immunol. *178*, 4112–4119.

Rubio, V., Stuge, T.B., Singh, N., Betts, M.R., Weber, J.S., Roederer, M., and Lee, P.P. (2003). Ex vivo identification, isolation and analysis of tumor-cytolytic T cells. Nat. Med. *9*, 1377–1382.

Seki, T., Yuasa, S., Oda, M., Egashira, T., Yae, K., Kusumoto, D., Nakata, H., Tohyama, S., Hashimoto, H., Kodaira, M., et al. (2010). Generation of induced pluripotent stem cells from human terminally differentiated circulating T cells. Cell Stem Cell *7*, 11–14.

Serwold, T., Hochedlinger, K., Inlay, M.A., Jaenisch, R., and Weissman, I.L. (2007). Early TCR expression and aberrant T cell development in mice with endogenous prerearranged T cell receptor genes. J. Immunol. *179*, 928–938.

Serwold, T., Hochedlinger, K., Swindle, J., Hedgpeth, J., Jaenisch, R., and Weissman, I.L. (2010). T-cell receptor-driven lymphomagenesis in mice derived from a reprogrammed T cell. Proc. Natl. Acad. Sci. USA *107*, 18939–18943.

Staerk, J., Dawlaty, M.M., Gao, Q., Maetzel, D., Hanna, J., Sommer, C.A., Mostoslavsky, G., and Jaenisch, R. (2010). Reprogramming of human peripheral blood cells to induced pluripotent stem cells. Cell Stem Cell *7*, 20–24.

Takahashi, K., Tanabe, K., Ohnuki, M., Narita, M., Ichisaka, T., Tomoda, K., and Yamanaka, S. (2007). Induction of pluripotent stem cells from adult human fibroblasts by defined factors. Cell *131*, 861–872.

Takayama, N., Nishikii, H., Usui, J., Tsukui, H., Sawaguchi, A., Hiroyama, T., Eto, K., and Nakauchi, H. (2008). Generation of functional platelets from human embryonic stem cells in vitro via ES-sacs, VEGF-promoted structures that concentrate hematopoietic progenitors. Blood *111*, 5298–5306.

Takayama, N., Nishimura, S., Nakamura, S., Shimizu, T., Ohnishi, R., Endo, H., Yamaguchi, T., Otsu, M., Nishimura, K., Nakanishi, M., et al. (2010). Transient activation of c-MYC expression is critical for efficient platelet generation from human induced pluripotent stem cells. J. Exp. Med. *207*, 2817–2830.

Tan, J.T., Ernst, B., Kieper, W.C., LeRoy, E., Sprent, J., and Surh, C.D. (2002). Interleukin (IL)-15 and IL-7 jointly regulate homeostatic proliferation of memory phenotype CD8+ cells but are not required for memory phenotype CD4+ cells. J. Exp. Med. *195*, 1523–1532.

Timmermans, F., Velghe, I., Vanwalleghem, L., De Smedt, M., Van Coppernolle, S., Taghon, T., Moore, H.D., Leclercq, G., Langerak, A.W., Kerre, T., et al. (2009). Generation of T cells from human embryonic stem cell-derived hematopoietic zones. J. Immunol. *182*, 6879–6888.

Tsunetsugu-Yokota, Y., Morikawa, Y., Isogai, M., Kawana-Tachikawa, A., Odawara, T., Nakamura, T., Grassi, F., Autran, B., and Iwamoto, A. (2003). Yeast-derived human immunodeficiency virus type 1 p55(gag) virus-like particles activate dendritic cells (DCs) and induce perforin expression in Gag-specific CD8(+) T cells by cross-presentation of DCs. J. Virol. *77*, 10250–10259.

Turka, L.A., Schatz, D.G., Oettinger, M.A., Chun, J.J., Gorka, C., Lee, K., McCormack, W.T., and Thompson, C.B. (1991). Thymocyte expression of RAG-1 and RAG-2: termination by T cell receptor cross-linking. Science *253*, 778–781.

Turtle, C.J., Swanson, H.M., Fujii, N., Estey, E.H., and Riddell, S.R. (2009). A distinct subset of self-renewing human memory CD8+ T cells survives cytotoxic chemotherapy. Immunity *31*, 834–844.

van Dongen, J.J., Langerak, A.W., Brüggemann, M., Evans, P.A., Hummel, M., Lavender, F.L., Delabesse, E., Davi, F., Schuuring, E., García-Sanz, R., et al. (2003). Design and standardization of PCR primers and protocols for detection of clonal immunoglobulin and T-cell receptor gene recombinations in suspect lymphoproliferations: report of the BIOMED-2 Concerted Action BMH4-CT98-3936. Leukemia *17*, 2257–2317.

Veldwijk, M.R., Berlinghoff, S., Laufs, S., Hengge, U.R., Zeller, W.J., Wenz, F., and Fruehauf, S. (2004). Suicide gene therapy of sarcoma cell lines using recombinant adeno-associated virus 2 vectors. Cancer Gene Ther. *11*, 577–584.

Virgin, H.W., Wherry, E.J., and Ahmed, R. (2009). Redefining chronic viral infection. Cell *138*, 30–50.

Vodyanik, M.A., Bork, J.A., Thomson, J.A., and Slukvin, I.I. (2005). Human embryonic stem cell-derived CD34+ cells: efficient production in the coculture with OP9 stromal cells and analysis of lymphohematopoietic potential. Blood *105*, 617–626.

von Boehmer, H. (2004). Selection of the T-cell repertoire: receptor-controlled checkpoints in T-cell development. Adv. Immunol. *84*, 201–238.

Watarai, H., Rybouchkin, A., Hongo, N., Nagata, Y., Sakata, S., Sekine, E., Dashtsoodol, N., Tashiro, T., Fujii, S., Shimizu, K., et al. (2010). Generation of functional NKT cells in vitro from embryonic stem cells bearing rearranged invariant Valpha14-Jalpha18 TCRalpha gene. Blood *115*, 230–237.

Weng, N.P., Hathcock, K.S., and Hodes, R.J. (1998). Regulation of telomere length and telomerase in T and B cells: a mechanism for maintaining replicative potential. Immunity *9*, 151–157.

Wherry, E.J. (2011). T cell exhaustion. Nat. Immunol. *12*, 492–499.

Zhang, N., and Bevan, M.J. (2011). CD8(+) T cells: foot soldiers of the immune system. Immunity *35*, 161–168.

JVI
Journals.ASM.org

Significant Reductions in Gag-Protease-Mediated HIV-1 Replication Capacity during the Course of the Epidemic in Japan

Shigeru Nomura,[a] Noriaki Hosoya,[b] Zabrina L. Brumme,[c,d] Mark A. Brockman,[c,d] Tadashi Kikuchi,[a] Michiko Koga,[a] Hitomi Nakamura,[a] Tomohiko Koibuchi,[e] Takeshi Fujii,[e] Jonathan M. Carlson,[f] David Heckerman,[f] Ai Kawana-Tachikawa,[a] Aikichi Iwamoto,[a] Toshiyuki Miura[a]*

Division of Infectious Diseases, Advanced Clinical Research Center, Institute of Medical Science, University of Tokyo, Tokyo, Japan[a]; Department of Infectious Disease Control, International Research Center for Infectious Diseases, Institute of Medical Science, University of Tokyo, Tokyo, Japan[b]; Faculty of Health Sciences, Simon Fraser University, Burnaby, British Columbia, Canada[c]; British Columbia Centre for Excellence in HIV/AIDS, Vancouver, British Columbia, Canada[d]; Department of Infectious Diseases and Applied Immunology, Institute of Medical Science, University of Tokyo, Tokyo, Japan[e]; Microsoft Research, Los Angeles, California, USA[f]

Human immunodeficiency virus type 1 (HIV-1) evolves rapidly in response to host immune selection pressures. As a result, the functional properties of HIV-1 isolates from earlier in the epidemic may differ from those of isolates from later stages. However, few studies have investigated alterations in viral replication capacity (RC) over the epidemic. In the present study, we compare Gag-Protease-associated RC between early and late isolates in Japan (1994 to 2009). HIV-1 subtype B sequences from 156 antiretroviral-naïve Japanese with chronic asymptomatic infection were used to construct a chimeric NL4-3 strain encoding plasma-derived *gag-protease*. Viral replication capacity was examined by infecting a long terminal repeat-driven green fluorescent protein-reporter T cell line. We observed a reduction in the RC of chimeric NL4-3 over the epidemic, which remained significant after adjusting for the CD4$^+$ T cell count and plasma virus load. The same outcome was seen when limiting the analysis to a single large cluster of related sequences, indicating that our results are not due to shifts in the molecular epidemiology of the epidemic in Japan. Moreover, the change in RC was independent of genetic distance between patient-derived sequences and wild-type NL4-3, thus ruling out potential temporal bias due to genetic similarity between patient and historic viral backbone sequences. Collectively, these data indicate that Gag-Protease-associated HIV-1 replication capacity has decreased over the epidemic in Japan. Larger studies from multiple geographical regions will be required to confirm this phenomenon.

It has been almost 30 years since the discovery of human immunodeficiency virus type 1 (HIV-1) (1), a pathogen that first infected human populations approximately 100 years ago (2, 3). Over the course of the pandemic, substantial and various selection pressures have been exerted on HIV-1 by its human host, possibly resulting in alterations in viral replication capacity (RC), virulence, and/or other properties (4). However, few studies to date have examined population-level alterations in HIV-1 replication capacity over the epidemic's course (5, 6), and none have investigated the potential role of immune escape mutations selected by cellular immune responses in modulating this phenomenon.

Cytotoxic T lymphocytes (CTLs) play a major role in controlling viremia and disease progression in HIV-1 infection (7–11). However, the selection of escape mutations within or near CTL epitopes facilitates viral immune evasion (12–16) and represents a major challenge for HIV vaccine design. Since CTL responses are restricted by human leukocyte antigen (HLA) class I alleles, CTL escape mutations emerge in an HLA-specific manner. Many CTL escape mutations have been identified experimentally (15, 17–20); moreover, statistical analyses of large population-level data sets have yielded HLA-associated mutation maps of HIV-1 protein sequences, thereby identifying putative CTL escape sites (21–27). Importantly, these escape variants may be transmitted both vertically and horizontally (12, 28, 29). Furthermore, CTL escape variants selected by common HLA class I alleles may have been accumulating at the population level over the course of the epidemic in some regions, most notably, Japan (30, 31). If this is the case, active CTL epitopes restricted by common HLA class I alleles may be lost through mutational escape as the epidemic matures, possibly leading to increased viral virulence through enhanced immune evasion in these populations.

Although CTL escape mutations allow HIV to evade immune detection, they can also reduce viral replication capacity (28, 32–38). Furthermore, while certain virus-attenuating escape mutations revert upon transmission to recipients lacking the relevant HLA class I allele (20, 28, 36), this is not always the case (39, 40). Indeed, a recent study suggested that fixation of viruses carrying such attenuating escape mutations is increasing in an allele frequency-dependent manner in certain populations (30). These observations have led to the hypothesis that the *in vitro* replication capacity of HIV-1 may have been decreasing over the epidemic's course in certain populations, at the expense of the loss of active CTL epitopes at the population level through mutational escape.

In the present study, we generated chimeric HIV-1 isolates by inserting plasma HIV RNA-derived *gag-protease* sequences from 156 asymptomatic, chronically infected treatment-naïve Japanese patients dating from 1994 to 2009 into a laboratory strain backbone (HIV-1 NL4-3) and examined their replication capacity using published methods (33, 41–44). We specifically focused on the

Received 24 August 2012 Accepted 5 November 2012
Published ahead of print 14 November 2012
Address correspondence to Toshiyuki Miura, toshiyuki.miura@gmail.com.
* Present address: Toshiyuki Miura, The Institute of Tropical Medicine, Nagasaki University, Nagasaki, and ViiV Healthcare K.K., Tokyo, Japan.

doi:10.1128/JVI.02122-12

TABLE 1 Demographic characteristics of the participants[a]

Characteristic	Value
Median (range) age (yr)	31 (18–73)
No. (%) of participants by gender	
Male	167 (94)
Female	10 (5.6)
Median (IQR) $CD4^+$ T cell count (no. of cells μl^{-1})	339 (269–452)
Median (IQR) pVL (no. of RNA copies/ml)	23,000 (5,700–46,000)
No. (%) of participants by route of transmission[b]	
Men who have sex with men	147 (83)
Heterosexual	25 (14)
Unknown	5 (2.8)

[a] Data are for 177 participants.
[b] Hemophilia patients were excluded from this study.

Gag protein, as it is likely to be the most important target of HLA-restricted CTLs (45) and because numerous fitness-reducing HLA-associated escape mutations have been described therein (28, 32–38). As such, Gag is ideal for investigating the potential effects of immune-mediated HIV attenuation over time. Overall, we have observed a significant reduction in Gag-Protease-mediated HIV-1 replication capacity as the epidemic has matured in Japan.

MATERIALS AND METHODS

Study participants. A total of 177 antiretroviral-naïve Japanese individuals with asymptomatic chronic HIV-1 infection who visited the Research Hospital of the University of Tokyo from April 1992 through March 2009 were enrolled. Individuals with acute HIV infection, chronically infected individuals with a history of AIDS-defining illnesses, and hemophilia patients were excluded (hemophilia patients were excluded because Japanese hemophiliacs acquired HIV-1 from imported blood products in the mid-1980s [46, 47], a fact which could confound our analyses). The sociodemographic characteristics of the participants are shown in Table 1. Blood collected at the earliest available time point during the asymptomatic chronic phase of infection (median, 173 days after diagnosis; interquartile range [IQR], 56 to 525 days after diagnosis; range, 0 to 4,313 days after diagnosis) was studied. Plasma and peripheral blood mononuclear cells (PBMCs) were separated by standard procedures and stored at −80°C and in liquid nitrogen, respectively, until use. The study was approved by the Institutional Review Board of the Institute of Medical Science, University of Tokyo. Written informed consent was obtained from all participants.

HLA class I typing. Genomic DNA was extracted from PBMCs using a QIAamp DNA blood minikit (Qiagen Inc., Valencia, CA) following the manufacturer's instructions. High-resolution HLA class I typing was performed using a WAKFlow HLA typing kit (Wakunaga, Hiroshima, Japan) and a Luminex multianalyte profiling system (Luminex Corporation, Austin, TX).

Viral RNA isolation. Plasma (500 μl) was quickly spun down to remove cell debris. The resulting clarified plasma was then centrifuged at 14,000 rpm (20,000 × *g*) for 120 min to pellet the virions. After centrifugation, 360 μl of the supernatant was discarded, leaving 140 μl plasma for which viral RNA was extracted using a QIAamp viral RNA minikit (Qiagen Inc., Valencia, CA). Extracted viral RNA was eluted in 80 μl of elution buffer and stored at −80°C until use.

Plasma virus sequencing. The HIV-1 *gag-protease* region was amplified from extracted plasma HIV RNA as described previously, with some modifications (48). We included *protease* since disruption of the autologous combination of Gag and Protease may negatively affect Protease-mediated cleavage of Gag protein products, thus compromising the RC of the recombinant viruses. Briefly, reverse transcriptase PCR (RT-PCR) was performed using a Superscript III one-step RT-PCR system with Platinum *Taq* DNA polymerase with high fidelity (Invitrogen, Carlsbad, CA). Each 50-μl reaction mixture was composed of 4 μl of viral RNA, 25 μl of 2× reaction mix, 200 nM forward and reverse outer primers, 1 μl of enzyme mix, and water. RT-PCR primer sequences were AAATCTCTAGCAGTG GCGCCCGAACAG (strain HXB2 nucleotide numbering, positions 623 to 649) for the forward primer and TAACCCTGCGGGATGTGGTA TTCC (positions 2849 to 2826) for the reverse primer. Thermal cycling conditions for the RT-PCR were 50°C for 30 min and 94°C for 2 min, followed by 35 cycles of 94°C for 15 s, 56°C for 30 s, and 68°C for 2 min. Second-round DNA PCR was performed using TaKaRa Ex *Taq* DNA polymerase Hot Start enzyme (TaKaRa Bio Inc., Shiga, Japan). Each reaction mixture contained 2 μl of the PCR product from the RT-PCR. PCR primer sequences were GCGGCGACTGGTGAGTACGCC (positions 734 to 754) for the forward primer and TCCTTTAGTTGCCCCCCTATC for the reverse primer (positions 2314 to 2294). Thermal cycling conditions were 94°C for 2 min, followed by 35 cycles of 94°C for 30 s, 60°C for 30 s, and 72°C for 2 min and, finally, 10 min at 68°C. To examine *protease* sequences, the *gag-protease* region was reamplified from existing 1st-round RT-PCR products using forward primer GCTAGAAGGAGAGAG ATGGG (positions 775 to 794 on HXB2) and reverse primer CAGTCTC AATAGGACTAATGGG (positions 2550 to 2571) with the same thermal cycler conditions described above. PCR amplifications were confirmed by agarose gel electrophoresis, and successful amplicons were purified using a QIAquick PCR purification kit (Qiagen Inc., Valencia, CA) according to the manufacturer's instructions. Population sequences were obtained by bidirectional reading using an ABI Prism BigDye Terminator (version 3.1) cycle sequencing kit (Applied Biosystems, Foster City, CA) on an Applied Biosystems 3130xl genetic analyzer. Chromatograms were edited using Sequencher software (Gene Codes Corporation, Ann Arbor, MI); nucleotide mixtures were called if the height of the secondary peak exceeded 25% of the dominant peak height. Multiple alignments were constructed using the ClustalW program. Maximum-likelihood phylogenetic trees were drawn from nucleotide alignments using DNAml of the PHYLIP program integrated into the BioEdit software package. HIV-1 subtypes were determined by the REGA HIV subtyping tool (http://hivdb.stanford.edu/). Recombinant viruses were detected using the recombination identification program (RIP; available at http://www.hiv.lanl.gov/content/sequence/RIP/RIP.html) and the jpHMM program (GOBICS; University of Göttingen). Pairwise genetic distances between individual *gag* sequences and the HIV-1 reference strain NL4-3 were calculated using DNAdist of the PHYLIP program integrated into BioEdit software.

Generation of chimeric viruses. Chimeric NL4-3 viruses were generated as previously described (33, 49). Briefly, the *gag-protease* region was reamplified from the 1st-round RT-PCR products using 100-bp-long primers homologous to the NL4-3 reference strain (forward primer, GAC TCG GCT TGC TGA AGC GCG CAC GGC AAG AGG CGA GGG GCG GCG ACT GGT GAG TAC GCC AAA AAT TTT GAC TAG CGG AGG CTA GAA GGA GAG AGA TGG G [positions 695 to 794 on HXB2]; reverse primer, ATG CTT TTA TTT TTT CTT CTG TCA ATG GCC ATT GTT TAA CTT TTG GGC CAT CCA TTC CTG GCT TTA ATT TTA CTG GTA CAG TCT CAA TAG GAC TAA TGG G [positions 2649 to 2550]). Note that the forward primer overlapped the *gag*-coding sequence by five bases (underlined), and the reverse primer ended one base downstream of the protease gene. The PCR was undertaken in a final volume of 100 μl, consisting of 4 μl of 10 μM forward and reverse primers, 90 μl of Invitrogen Platinum PCR SuperMix high fidelity (Invitrogen, Carlsbad, CA), and 2 μl of the RT-PCR product. Thermal cycling conditions were 95°C for 2 min, followed by 35 cycles of 94°C for 30 s, 65°C for 30 s, and 72°C for 2 min and a 7-min extension of 72°C. PCR products were purified with the QIAquick PCR purification kit (Qiagen Inc., Valencia, CA) and eluted in 50 μl of elution buffer. pNL4-3 with a *gag-protease* deletion (33) and 5 to 10 μg of purified PCR product were cotransfected into 2.5×10^6 cells of a long terminal repeat (LTR)-driven green fluorescent protein (GFP)-reporter T cell

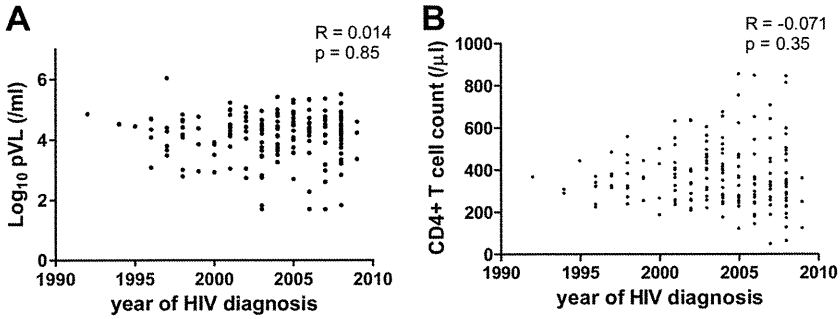

FIG 1 Correlation between plasma virus load, $CD4^+$ T cell count, and year of HIV-1 diagnosis. No significant correlation between plasma HIV-1 load and the year of diagnosis (A) or the $CD4^+$ T cell count and the year of diagnosis (B) was observed. Plasma virus loads and $CD4^+$ T cell counts are based upon a single time point (date of blood sampling). Each dot represents a single individual (n = 177).

line (GXR cells, CEM origin [50]) in 800 μl of R10+ medium (RPMI medium with 10% fetal calf serum containing penicillin and streptomycin) by electroporation (exponential protocol, 300 V, 500 μF). Cells were incubated for 45 min at room temperature, subsequently transferred to T25 flasks in 10 ml of R10+ medium, and incubated at 37°C with 5% CO_2. GFP expression was monitored by flow cytometry (FACSCalibur; BD Biosciences, San Jose, CA) every 1 to 2 days after day 5. Supernatants containing recombinant virus stocks were harvested after GFP expression reached 15% among viable cells, and 1-ml aliquots were stored at −80°C until use. To verify the patient origin of each recombinant virus stock and rule out contamination or sample mix-up, viral RNA was extracted from 30 μl of virus stock using a ChargeSwitch EasyPlex viral kit (Invitrogen, Carlsbad, CA). *gag* sequences were obtained using the same method used for plasma virus sequencing described earlier, and maximum-likelihood phylogenetic trees incorporating the original bulk and recombinant virus sequences were constructed using DNAml.

Determination of recombinant virus titers and RC assay. Determination of the titers of recombinant virus stocks and viral RC assays were performed as described previously (32, 35, 48, 50, 51). For determination of viral titer, 400-μl viral stocks were mixed with 1.0×10^6 GXR cells in 100 μl of R10+ medium in a 24-well plate and incubated at 37°C with 5% CO_2. After 24 h, 1 ml R10+ medium was added to each culture. After 48 h, the titers of virus stocks were determined by measuring the percentage of GFP-positive (GFP^+) cells using flow cytometry. In the subsequent replication capacity assay, virus stocks were used to infect 1.0×10^6 GXR cells at a multiplicity of infection of 0.002 in 500 μl of R10+ medium in a 24-well plate. All assays included a positive (wild-type NL4-3) and a negative (cells-only) control. Assay mixtures were incubated overnight at 37°C with 5% CO_2, and 1 ml of R10+ medium was added on the following day (day 1). The percentage of GFP^+ cells was then measured by flow cytometry every other day for the following week (days 2 to 8). For each virus, the natural log slope of the percentage of GFP^+ cells was calculated during the exponential phase of viral spread (days 2 to 6). This value was divided by the mean rate of spread of the wild-type NL4-3 control to generate a normalized, quantitative measure of RC. An RC value of 1.0 indicates a rate of viral growth that was equal to that of NL4-3, while RC values of <1.0 and >1.0 indicate rates of spread that were lower and higher than the rate for wild-type NL4-3, respectively. All viruses were tested in a single experiment by a single operator; this experiment was performed in triplicate using fresh viral stocks for each one. Final RC values therefore represent the averages of wild-type NL4-3-normalized triplicate measurements.

Statistical analysis. Statistical comparisons between independent groups were performed using the Mann-Whitney U test. Univariate correlation analysis was performed using Spearman's correlation. Multiple-regression analyses were performed using standard least-squares methods. For these analyses, a P value of <0.05 was considered significant. Analyses were performed in GraphPad Prism (version 5.03) software (GraphPad Software, La Jolla, CA).

Published phylogenetically informed methods were used to identify amino acids in Gag and Protease significantly associated with HLA class I alleles expressed in our data set (52, 53). Associations between viral RC and specific amino acid residues within Gag and Protease observed with a minimum frequency of 3 were identified using the Mann-Whitney U test. In these analyses, multiple comparisons were addressed using q values, the P value analogue of the false discovery rate (FDR) (54). The FDR is the expected proportion of false positives among results deemed significant at a given P-value threshold; for example, at a q value of ≤0.2, we expect 20% of identified associations to be false positives.

Nucleotide sequence accession numbers. *gag* and *protease* sequences have been submitted to GenBank (accession numbers JX264247 to JX264562).

RESULTS

No significant temporal changes in $CD4^+$ T cell count or pVLs by year of HIV-1 diagnosis. A total of 177 asymptomatic, chronically HIV-1-infected Japanese individuals were enrolled. Since the replicative capacity of viruses within an individual's quasispecies tends to increase over the infection course (55–58) and immune-driven selection in Gag by protective HLA alleles predominantly affects viral RC in acute/early infection (44), individuals with acute infection and those with a history of AIDS-defining illnesses were excluded. Clinical markers of HIV infection ($CD4^+$ T cell count and plasma virus loads [pVLs] at the time of sampling) were comparable among subjects, despite differences in year of HIV diagnosis (Fig. 1). Furthermore, although the timing of blood sampling varied substantially between subjects, no correlation between diagnosis year and the duration from diagnosis to blood sampling was observed (data not shown; R = 0.0084, P = 0.92).

Relationship between viral replication capacity and clinical markers of HIV infection. Of the 177 enrolled patients, full-length amplification of *gag-protease* was successful for 168 of these (94.9%). Eight individuals infected with non-clade B viruses (6 infected with CRF01_AE, 1 with CRF02_AG, and 1 with A1) and two individuals with intersubtype clade B *gag* recombinants were excluded from study. After construction of chimeric viral stocks and confirmation of their patient origin (Fig. 2), a further two samples were excluded due to suspected contamination. Viral RC was thus assessed for the remaining 156 recombinant viruses. Each recombinant virus was used to infect a GFP reporter T cell line, and its *in vitro* RC was examined over a 7-day period. Since

FIG 2 Validation of the origin of the *gag-protease* region in chimeric NL4-3 viruses. To verify the patient origin of each chimeric virus, a maximum-likelihood phylogenetic tree was constructed using plasma (red) and chimeric (blue) *gag* sequences. This tree includes 156 validated chimeric viruses that clustered with their original bulk sequences (two viruses were removed due to suspected contamination). The tree is rooted using the HIV-1 subtype A1 reference strain with GenBank accession number AF004885.

the set-point viral load has been associated with the *in vitro* replication of chimeric viruses (33, 42, 43, 55–59), we first examined the potential correlation between plasma viral load, $CD4^+$ T cell count, and RC of chimeric NL4-3 strains. A significant positive correlation between RC and plasma virus load was observed ($R = 0.21$, $P = 0.0072$; Fig. 3A), consistent with previous reports of the reduced RC of chimeric NL4-3 derived from HIV-1 controllers (33, 41, 42). No significant correlation between $CD4^+$ T cell count and RC was observed ($R = -0.042$, $P = 0.60$; Fig. 3B), possibly due to exclusion of individuals with advanced disease from the present study.

Change in Gag-Protease-associated viral replication capacity over the epidemic in Japan. In order to investigate temporal changes in viral RC over the epidemic in Japan, the correlation between RC and year of HIV diagnosis was analyzed, revealing a significant inverse correlation ($R = -0.27$, $P = 0.0006$; Fig. 4A). This observation remained statistically significant in a multivariate linear regression model adjusting for $CD4^+$ T cell count and plasma virus load ($P = 0.0008$; partial regression coefficients, -0.0064; 95% confidence interval [CI], -0.0101 to -0.0027). Consistent results were obtained when the original analysis was stratified by $CD4^+$ T cell count at blood sampling (for CD4 T cell

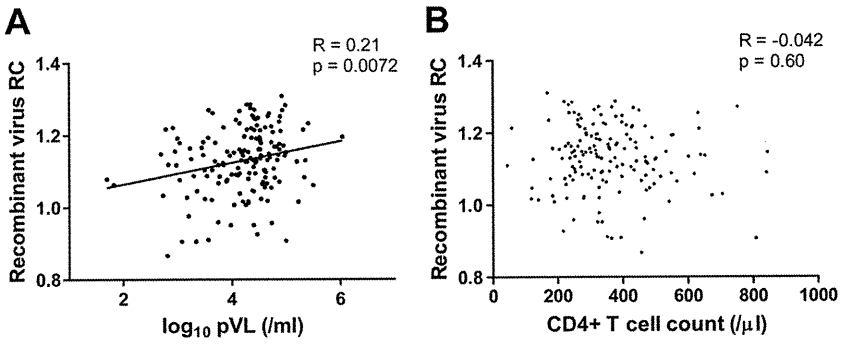

FIG 3 Correlation between replication capacity of chimeric NL4-3 and clinical markers of HIV infection. The correlation of replication capacity of chimeric NL4-3 with pVL (A) and CD4 T cell count (B) at the time of blood sampling ($n = 156$) is shown. A statistically significant positive correlation between RC and pVL was observed ($R = 0.21$, $P = 0.0072$).

counts of >200, $R = -0.28$ and $P = 0.0009$; for CD4 T cell counts of >300, $R = -0.25$ and $P = 0.013$; for CD4 T cell counts of >500, $R = -0.39$ and $P = 0.080$; Fig. 4B to D). Taken together, these results support a decline in Gag-Protease-mediated RC in HIV-1 over the course of the Japanese epidemic which is independent of differences in pVLs and CD4 T cell counts in the studied population. Since the duration from HIV diagnosis to blood sampling varied among the subjects, the analysis was repeated and was lim-

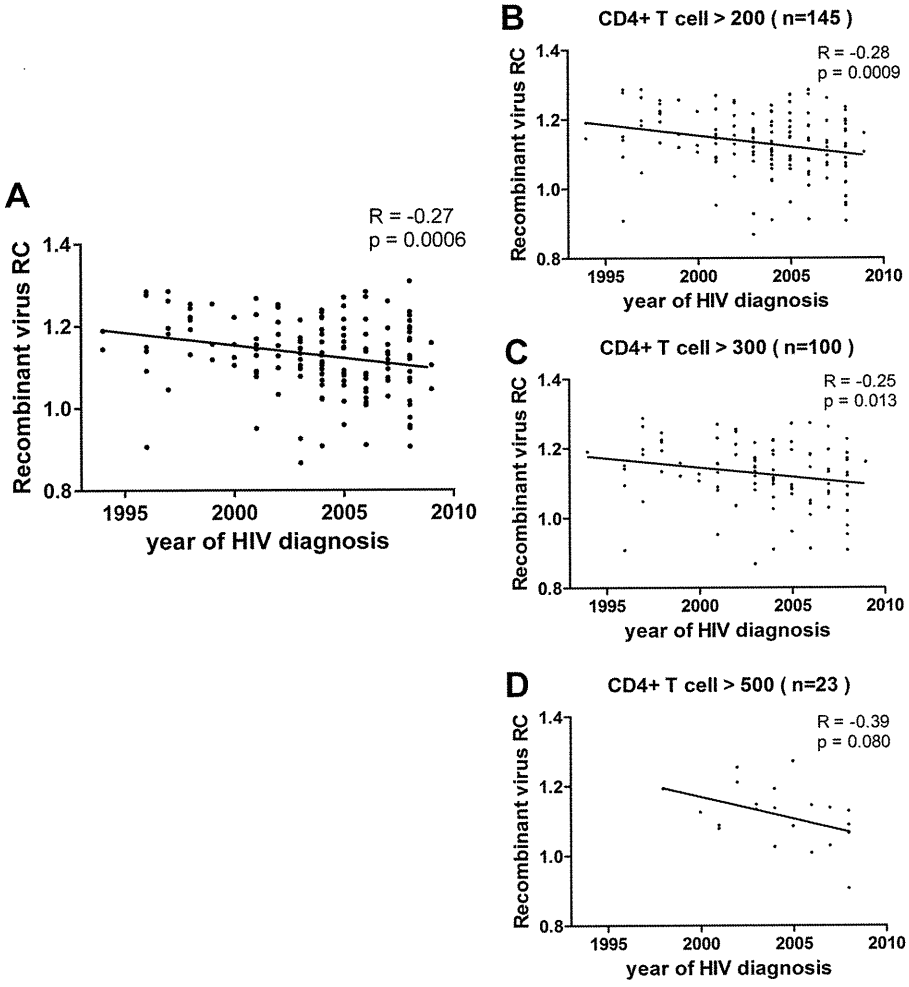

FIG 4 Change in Gag-Protease-associated viral replication capacity over the epidemic in Japan. A statistically significant inverse correlation between year of diagnosis and replication capacity was observed in all subjects regardless of CD4 T cell count ($n = 156$) (A), only in subjects with a $CD4^+$ T cell count of >200/μl ($n = 145$) (B), and only in subjects with a $CD4^+$ T cell count of >300/μl ($n = 100$) (C). A similar tendency was observed when the analysis was limited to subjects with a $CD4^+$ T cell count of >500/μl ($n = 23$) (D).

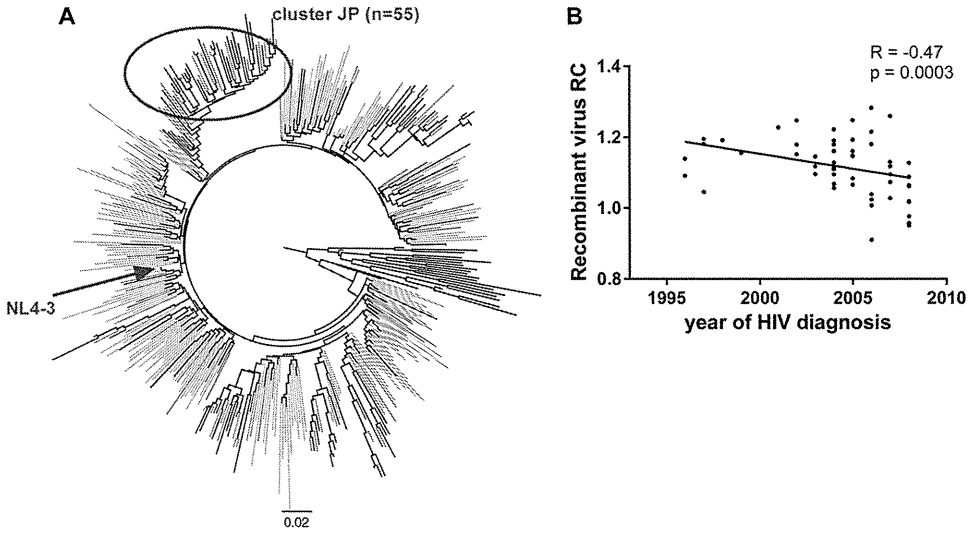

FIG 5 Temporal change in Gag-Protease-associated viral replication capacity of 55 sequences from a phylogenetic cluster. (A) Maximum-likelihood phylogenetic tree constructed using *gag* sequences from 156 Japanese individuals obtained in the present study and 263 individuals from other countries (randomly selected from the Los Alamos National Laboratory HIV sequence database). Purple, light blue, and blue branches, Japanese sequences with HIV diagnoses of 1999 or earlier, 2000 to 2004, and 2005 or later, respectively; green branches, sequences from the United States and Canada; yellow branches, sequences from other countries (Argentina, Australia, Brazil, China, Cuba, Cyprus, Denmark, France, Germany, Hong Kong, India, Italy, Jamaica, Myanmar, Netherlands, Russia, South Africa, South Korea, Spain, Taiwan, Thailand, and the United Kingdom). Reference strains (which include two reference sequences for each of the HIV-1 group M subtypes, as well as inferred ancestral sequences of the A, B, and C subtypes [obtained from the Los Alamos National Laboratory database]) are shown in black. NL4-3 is shown as red. The tree is rooted using the HIV-1 subtype A1 reference strain with GenBank accession number AF004885. A large cluster of Japanese sequences ($n = 55$) is indicated by the large red circle. (B) A significant inverse correlation between the replication capacity of chimeric viruses and year of HIV diagnosis for the viruses within this large Japanese cluster ($n = 55$).

ited to the subjects whose blood collection had been performed within a year of diagnosis of HIV infection; however, the inverse correlation remained significant ($n = 105, R = -0.25, P = 0.0080$; data not shown).

A potential confounder in such analyses is the molecular epidemiology of the epidemic itself. Theoretically, if distinct subtype B lineages with differential replication capacities were introduced into Japan at different times during the study period, this could influence our results. In order to exclude this possibility, we constructed a phylogenetic tree featuring global HIV-1 subtype B sequences (retrieved from the HIV sequence database at Los Alamos National Laboratory). Multiple clusters of Japanese clade B sequences were interspersed throughout the tree; however, all clusters contained sequences spanning the entire study period, indicating that there have been no major intraclade shifts within Japan in the past 2 decades (Fig. 5A). To further address this issue, we restricted our analysis to one particularly large cluster containing 55 sequences sampled over the study period (Fig. 5A) and found that the significant inverse correlation between RC and the year of diagnosis remained highly statistically significant in this cluster ($R = -0.47$, $P = 0.0003$; Fig. 5B). Taken together, these results support a decline in Gag-Protease-mediated RC in HIV-1 over the course of the Japanese epidemic which is not likely explained by shifts in the molecular epidemiology of HIV-1 over the period studied.

No correlation between replication capacity of chimeric viruses and their genetic distance from wild-type strain NL4-3. Chimeric NL4-3 virus carrying *gag-protease* derived from subtype C isolates (42, 43) displayed reduced RC compared to viruses derived from subtype B, likely due in part to the substantial genetic distance between insert and backbone. It is therefore conceivable that subtype B sequences sampled from the early part of the epidemic may be more similar to the NL4-3 backbone sequence (first characterized in 1986 [60]) than those sampled later and that this may influence RC. To investigate this potential confounder, we calculated the genetic distance between each patient isolate and the wild-type NL4-3 *gag* sequence, and we examined the correlation between genetic distance and viral RC. No such relationship was observed ($R = 0.0015$, $P = 0.98$; Fig. 6). Moreover, RC of chimeric viruses remained inversely correlated with the year of HIV diagnosis in multivariate analyses controlling for genetic distance from NL4-3 ($P = 0.0001$; partial regression coefficients, -0.0086; 95% CI, -0.0129 to -0.0044). It is therefore reasonable

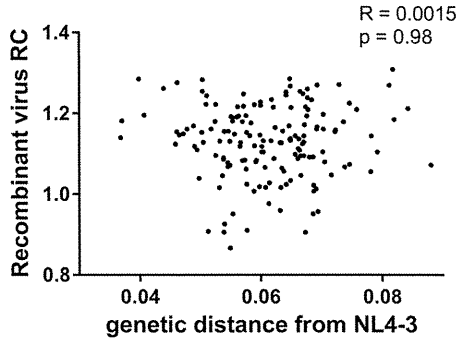

FIG 6 Chimeric virus replication capacity is not related to genetic distance between the insert and backbone. Pairwise genetic distances between the *gag* nucleotide sequence of each insert (clinical isolate sequence) and backbone (wild-type NL4-3) were calculated as described in Materials and Methods. No statistically significant correlation between the genetic distance and replication capacity of chimeric NL4-3 was observed.

to conclude that the decline in Gag-Protease-associated viral RC observed over the epidemic in Japan is unlikely to be explained by gross genetic incompatibility between NL4-3 and later clinical sequences circulating in the Japanese population.

Accumulation of PI resistance-associated mutations over time? Twelve major protease inhibitor (PI) resistance-associated mutations have been reported in the HIV Drug Resistance Database at Stanford University (http://hivdb.stanford.edu/), and some of these reduce viral replication capacity (61–67). To address the temporal accumulation of PI resistance mutations as a potential confounder, HIV-1 *protease* sequences were examined for 140 subjects for whom chimeric viruses were generated (for the remaining 15 patients, PCR or sequencing was unsuccessful). PI resistance-associated mutations were observed in 6 subjects, none of whom carried more than one PI resistance-associated mutation (4 were M46L and 2 were N88S), and all but 1 were enrolled after 2005. The median RC of chimeric NL4-3 derived from subjects with these PI resistance-associated mutations ($n = 6$) was higher than that of the others ($n = 134$) (1.21 versus 1.13; $P = 0.013$). Moreover, after excluding viruses derived from these 6 subjects from the original analysis, the temporal decline in chimeric virus RC remained significant ($R = -0.33$, $P < 0.0001$). Collectively, these data indicate that accumulation of PI resistance-associated variants in the population does not explain the change in viral RC over time in Japan.

Relationship between HLA class I alleles and temporal change in replication capacities of chimeric viruses. Chimeric NL4-3 virus derived from recent patient sequences displayed reduced *in vitro* RC compared to earlier isolates. To investigate whether immune selection pressure by specific HLA class I alleles could have contributed to this relative attenuation, the RCs of chimeric viruses were compared with respect to the presence versus absence of particular HLA-A, -B, and -C alleles in their host (note that analyses were limited to HLA alleles expressed in >20 individuals). In a cross-sectional analysis undertaken on the whole cohort regardless of sampling date, no significant associations between HLA class I expression and viral RC were observed (data not shown). However, when recombinant viruses were stratified on the basis of the year of HIV diagnosis (2002 or earlier versus 2003 or later), significantly lower median RC values were observed among A*24-expressing persons in early stages (for A*24-positive [$A*24^+$] versus A*24-negative [$A*24^-$] persons, 1.14 versus 1.21; $P = 0.024$) but not later stages (for $A*24^+$ versus $A*24^-$ persons, 1.12 versus 1.11; $P = 0.20$) of the epidemic (Fig. 7A), suggesting that the viral RC in $A*24^-$ persons in the early stage might have declined to levels comparable to those of $A*24^+$ persons in the late stage. Such a phenomenon was not observed for other HLA class I alleles (the results for A*02, B*40, and C*03 are shown in Fig. 7B to D, respectively). Nearly 70% of Japanese express HLA-A*24, making it the most common class I allele in this population. Our finding raises the intriguing hypothesis that A*24-associated escape mutations, alone or in combination, reduce viral RC to a modest extent and that these A*24-attenuated viruses have increased in prevalence at the population level over the course of the Japanese epidemic via transmission to and persistence in non-A*24-expressing persons.

Due to the relative rarity of this allele in Caucasians and Africans, HLA-A*24-restricted CTL epitopes have not been studied extensively; nevertheless, two optimal A*24 CTL epitopes within Gag and Protease have been reported: KW9 in p17 (Gag positions 28 to 36) (68) and RL11 in p24 (Gag positions 294 to 304) (69). However, we observed no accumulation of particular mutations within either of these known epitopes (data not shown). A published *in silico* analysis undertaken on >1,500 subtype B-infected individuals from Canada, the United States, and Australia reported a putative escape association between HLA-A*24 and the K30R substitution in $p17^{Gag}$ (21). However, the accumulation of K30R was not observed in the present study (data not shown), and the RCs of chimeric viruses with this substitution were not statistically different from the RCs of those without it. In addition, a phylogenetically corrected analysis of HLA-associated polymorphisms in 156 Japanese viral sequences from the present study identified Gag V362I to be significantly associated with HLA-A*24 (present in 17% of $A*24^+$ patients versus 4.1% of $A*24^-$ patients; $P < 0.001$, $q < 0.1$). However, as this substitution was observed in only 3 of 74 A*24-negative individuals in the present study, it was not possible to demonstrate its accumulation over the study period.

Accumulation of mutations associated with reduced replication capacity. Lastly, we conducted an exploratory analysis to identify specific amino acids in Gag and Protease associated with viral RC in our data set. Although no associations were observed at a q value of <0.2, 34 amino acids within Gag and 5 within Protease were identified as being associated with a lower RC at a P value of <0.05 (all q values were <0.4; not shown). We then investigated whether the frequencies of viruses carrying these Gag or Protease mutations increased over the course of the epidemic. Of the 34 polymorphisms identified in Gag, 6 significantly increased over the study period (V46L, L64I, D121G, A224P, T470A, I479L), while of the 5 mutations identified in Protease, 1 (R41K) significantly increased over the study period. However, with the exception of Gag L64I (reported to be associated with A*68) (21), none of these polymorphisms are known to be HLA associated.

DISCUSSION

In the present study, we observed a significant reduction in Gag-Protease-associated HIV-1 replication capacity over the past 15 years of the HIV-1 epidemic in Japan.

Our analyses addressed a number of potential confounders. First, viral RC is known to change over the course of HIV infection (70, 71). Examining the RCs of viruses isolated from acutely infected subjects is therefore ideal; however, the availability of such historic panels of specimens from a particular geographical area is extremely limited. Therefore, to rule out infection stage as a potential confounder, we undertook multivariate analyses adjusting for CD4 count and pVL as surrogate markers of disease stage. Second, to exclude the possibility that the molecular epidemiology of HIV in Japan differed in the early and late phases of the epidemic, we performed a subanalysis limited to a particularly large cluster composed of only Japanese clade B sequences sampled over the study period. Lastly, to address a concern about incompatibility between backbone NL4-3 and *gag-protease* from recent clinical isolates, we demonstrated that the year of HIV diagnosis correlated with RC independently of the genetic distance between patient-derived sequences and the wild-type NL4-3 sequence. In all cases, our original findings still held after controlling for these potential confounders. Furthermore, temporal trends in RC did not appear to be driven by protease inhibitor resistance mutations (which were infrequent in the studied population). Nevertheless, we cannot rule out the possibility that the introduction of increas-

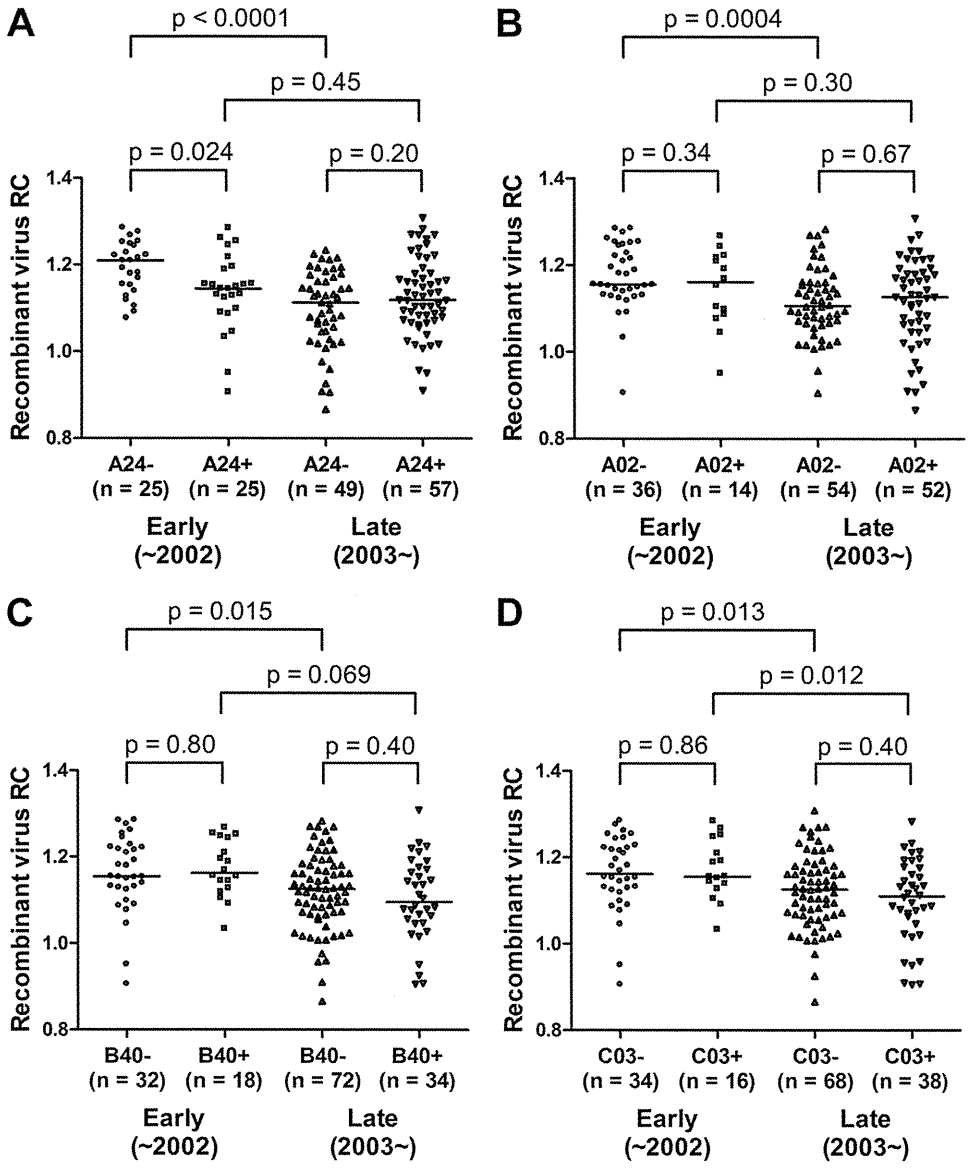

FIG 7 Relationship between common HLA alleles and chimeric virus replication capacity during early and late epidemic periods. To examine the potential impact of selection pressures by common HLA alleles in the Japanese population on the change in viral replication capacity, chimeric viruses were grouped according to year of HIV diagnosis (early [2002 or earlier] and late [2003 or later]), and associations between replication capacity and expression of particular HLA class I alleles were examined. Recombinant viruses from HLA-A*24-expressing hosts exhibited reduced RC before 2002 but not thereafter (A). However, such a phenomenon was not observed for other alleles investigated: A*02, B*40, and C*03 (B to D). Horizontal bars indicate the median values.

ingly more potent protease inhibitors over time is driving the selection of novel secondary drug resistance-associated polymorphisms that compromise RC and that such polymorphisms may be increasing in frequency in the general population.

Attempts have been made to study population-level changes in plasma HIV loads, CD4 T cell counts, and rates of disease progression over time as indirect evidence for altered HIV virulence over the epidemic's course. However, the lack of historic data, inherent limitations in conducting observational studies, and changes in the technologies used to measure clinical parameters have made this an extremely difficult issue to address. Despite this, a pattern appears to be emerging. While studies undertaken prior to the mid-1990s yielded conflicting results (72–76), more recent reports support the observation that HIV may be increasing in virulence as the epidemic progresses (77–85).

At first, published reports of increased virulence over time may appear to be inconsistent with our findings of reduced *in vitro* viral RC over the course of the Japanese epidemic. However, it is important to note that *in vitro* RC does not necessarily equate with viral virulence, as the former assesses the ability of a recombinant virus to replicate in a controlled *in vitro* environment devoid of host or other selection pressures, while the latter reflects the far more complex capacity of the virus to cause disease in its host. Indeed, while certain immune escape mutations reduce *in vitro* viral RC (28, 32–38), we must also consider that mutants with such escape mutations are highly adapted to their *in vivo* environ-